DMD Fast Forward. Published on December 10, 2021 as DOI: 10.1124/dmd.121.000695
This article has not been copyedited and formatted. The final version may differ from this version.

DMD-MR-2021-000695

Cynomolgus Monkey as an Emerging Animal Model to Study Drug Transporters: In Vitro, In Vivo, In Vitro-To-In Vivo Translation

Hong Shen, Zheng Yang, and A. David Rodrigues

Pharmaceutical Candidate Optimization, Bristol Myers Squibb Research & Development, Princeton, NJ USA (H.S. and Z. Y.) and ADME Sciences, Medicine Design, Worldwide Research & Development, Pfizer Inc., Groton CT USA (A.D.R.)

Running title: Cynomolgus monkey transporter models

Corresponding authors and contact information:

Dr. Hong Shen, Scientific Associate Director

Drug Metabolism and Pharmacokinetics (DMPK) Department

Bristol Myers Squibb Company

Route 206 & Province Line Road, Princeton, NJ 08543

Email: hong.shen1@bms.com

Phone: 609-252-4509

Fax : 609-252-6802

Number of text pages: 43

Number of tables: 5

Number of figures: 4

Number of references: 104

Number of words:

Abstract: 206

Abbreviations: ADME, absorption, distribution, metabolism, and excretion; *AUC*, area under plasma concentration-time curve; BBB, blood-brain barrier; BCRP, breast cancer resistance protein; BDC, bile duct cannulated; *CL*, clearance; CL_r, renal clearance; CYP, cytochrome P450; C_{max}, maximum plasma concentration; CP, coproporphyrin; DDI, drug-drug interaction; f_a, fraction absorbed; EMA, the European Medicines Agency; f_g, intestinal availability; f_h, hepatic

availability); FDA, US Food and Drug Administration; GFR, glomerular filtration rate; HEK293, human embryonic kidney 293 cells; IC_{50}, half-maximal inhibitory concentration; IVIVE, in vitro-to-in vivo extrapolation; K_i, inhibition constant; K_m, Michaelis-Menton constant; LC-MS/MS, liquid chromatography–tandem mass spectrometry; MATE, multidrug and toxin extrusion; MDCK, Madin-Darby canine kidney cell; MDR1, multidrug resistance protein 1; MRP, multidrug resistance-associated protein; NME, new molecular entity; NTCP, sodium-taurocholate cotransporting polypeptide; OAT, organic anion transporter; OATP, organic anion transporting polypeptide; OCT, organic cation transporter; P-gp, P-glycoprotein; PBPK, physiologically-based pharmacokinetic; PDA, pyridoxic acid; PK, pharmacokinetics; PXR, pregnane X receptor; *R*-value, ratio of victim AUC in the presence and absence of perpetrators (inhibitors or inducers) predicted with basic models; RT-PCR, reverse transcription polymerase chain reaction; $T_{1/2}$, terminal half-life; V_{max}, maximal transport rate; V_{ss}, steady-state volume of distribution; UGT, UDP-glucuronosyltransferase.

ABSTRACT

Membrane transporters have been recognized as one of the key determinants of pharmacokinetics and are also known to affect the efficacy and toxicity of drugs. Both qualitatively and quantitatively, however, transporter studies conducted using human in vitro systems have not always been predictive. Consequently, researchers have utilized cynomolgus monkeys as a model to study drug transporters and anticipate their effects in humans. Burgeoning reports of data in the last few years necessitates a comprehensive review on the topic of drug transporters in cynomolgus monkeys that includes cell-based tools, sequence homology, tissue expression, in vitro studies, in vivo studies, and in vitro-to-in vivo extrapolation (IVIVE). This review highlights the state-of-the-art applications of monkey transporter models to support the evaluation of transporter-mediated drug-drug interactions, clearance predictions, and endogenous transporter biomarker identification and validation. The data demonstrate that cynomolgus monkey transporter models, when used appropriately, can be an invaluable tool to support drug discovery and development processes. Most importantly, they provide an early IVIVE assessment which provides additional context to human in vitro data. Additionally, comprehending species similarities and differences in transporter tissue expression and activity is crucial when translating monkey data to humans. The challenges and limitations when applying such models to inform decision-making must also be considered.

SIGNIFICANCE STATEMENT

This paper presents a comprehensive review of currently available published reports describing cynomolgus monkey transporter models. The data indicate that cynomolgus monkeys provide mechanistic insight regarding the role of intestinal, hepatic, and renal transporters in drug and biomarker disposition and drug interactions. It is concluded that the data generated with cynomolgus monkey models provide mechanistic insight regarding transporter-mediated absorption and disposition, as well as human clearance prediction, drug-drug interaction assessment, and endogenous biomarker development related to drug transporters.

INTRODUCTION

It is now clear that drug transporters play an essential role in pharmacokinetics (PK) and affect the safe and effective use of drugs (Mizuno et al., 2003, International Transporter et al., 2010, Lee et al., 2017). There are numerous drug transporters expressed on the apical or basolateral membranes of polarized enterocytes, hepatocytes, renal proximal tubule epithelial cells, and the endothelial cells at the blood-brain barrier (BBB) that serve as the determinants of drug absorption and disposition. In agreement, an appreciable fraction of the human genome (i.e., approximately 10% or 1,600 to 2,000 genes) is assumed to be transporter-related (Hediger et al., 2013, Ye et al., 2014) and it is widely accepted that uptake and efflux transporters function together to mediate the vectorial transfer of drugs and endogenous compounds across polarized cell monolayers. The transporters governing the transmembrane movement of drugs are subdivided into two major superfamilies: ATP (adenosine triphosphate)-binding cassette (ABC) transporter superfamily that provides efflux functions and solute carriers (SLC) superfamily that are involved in both cellular influx and/or cellular efflux of drugs. To date, there are approximately 50 ABC and 400 SLC transporter genes that have been identified (Sheps and Ling, 2007, Kanehisa et al., 2010, Hediger et al., 2013, Shen et al., 2019b). While many transporters are part of the cellular homeostasis of critical substances such as amino acids, oligopeptides, nucleotides, vitamins, sugars, bile acids, and hormones, the *ABCB*, *ABCG*, *SLC22A*, *SLC47A*, and *SLCO1B* are common subfamilies that constitute major players in drug disposition (International Transporter et al., 2010). Inter-individual variations in tissue expression levels and transport activities caused by genetic, therapeutic, disease and environmental factors have been shown to contribute to the observed PK and pharmacodynamic (PD) variability across subjects, clinical cohorts, and populations. Consequently, the same drug

DMD Fast Forward. Published on December 10, 2021 as DOI: 10.1124/dmd.121.000695
This article has not been copyedited and formatted. The final version may differ from this version.

transporters are listed by the US Food and Drug Administration (FDA) and European Medicines Agency (EMA) for evaluation in DDI studies (https://www.fda.gov/media/134582/download and https://www.ema.europa.eu/en/documents/scientific-guideline/guideline-investigation-drug-interactions-revision-1_en.pdf). However, despite the growing knowledge in drug transporters in the last two decades, the extrapolation of in vitro data to clinical findings and prediction of transporter-mediated drug PK and drug-drug interactions (DDI) are less successful compared with drug-metabolizing enzymes. The mechanistic static approaches recommended by regulatory agencies are conservative by design, erring on the side of caution in transporter DDI prediction with a high false-positive rate. Overlapping substrate specificity and the redundant function of transporters, nonoptimal experimental conditions, and unknown perpetrator drug concentrations at the site of transporter interactions likely contribute to such high-false positive prediction rates. In addition, complex dynamic transporter-enzyme interplay also leads to difficulty in predicting drug PK, disposition, and DDI. Animal models may be utilized to evaluate the in vivo role of transporters in drug disposition and DDI (Tang and Prueksaritanont, 2010, Peters et al., 2016). As described in the following sections, the major drug transporter genes in cynomolgus monkeys share a high degree of similarity in amino acid sequence with their human counterparts (i.e., > 90%) (Tables 1 and 2). Additionally, it has been observed that cynomolgus monkey transporter function (substrate specificity and inhibition potency) is also similar to that of humans (Figures 3 and 4). This generates the hypothesis that the cynomolgus monkey is a relevant nonclinical model for human drug transporters and provides an appropriate in vivo context when interpreting in vitro data. Indeed, a vast amount of literature has emerged attempting to validate the cynomolgus monkey as an animal model to study drug transporters, especially to assess drug transporter inhibition in the last ten years. The hopes are particularly high in applying

cynomolgus monkey models for the investigation of transporter-mediated drug disposition and DDI, where plasma, urine, feces, and tissue samples can be more easily obtained during preclinical discovery and development. Despite the importance and progress of using cynomolgus monkeys as a model for drug transporter research, there are no reviews yet of this topic. Therefore, this review focuses on several aspects related to cynomolgus monkey transporter models and compares them with humans. These include monkey transporter homology, tissue expression, in vitro and in vivo activity, and DDI. Finally, the applications of cynomolgus monkey transporter models in drug discovery and development will be discussed in detail to demonstrate their impact.

DMD Fast Forward. Published on December 10, 2021 as DOI: 10.1124/dmd.121.000695
This article has not been copyedited and formatted. The final version may differ from this version.

COMPARISON OF CYNOMOLGUS MONKEY AND HUMAN DRUG TRANSPORTERS

(A) Overview of Cynomolgus Monkey Transporter Models

Monkeys are established as a nonclinical species for testing PK, PD, and safety, along with rodents, dogs, and other specialized species (Tang and Prueksaritanont, 2010, Deng et al., 2011, Uno et al., 2011). Monkeys are used because they possess many genetic, physiological, biochemical, and pharmacological similarities to humans. It is generally presumed that the similarities make the use of monkeys in nonclinical research a considered decision (Table 1). To date, only a few monkey species, such as macaques of the *Cercopithecidae* family are available and established as translational models for drug research. These primates share a common ancestor with humans, which is reported to have lived approximately more than 30 million years ago (Perelman et al., 2011). From this family, the species *Macaca fascicularis* and *Macaca mulatta*, also known as cynomolgus and rhesus monkeys, respectively, are the most common and best-studied nonhuman primate animal models today (Ebeling et al., 2011). However, usage of rhesus monkeys in drug testing has declined since India banned all rhesus monkey exports to breeding centers across the world. As an alternative to the rhesus, several commercial breeding centers in Indonesia, China, the Philippines, and Mauritius tried to provide a sufficient number of captive-bred cynomolgus monkeys originating from wild-trapped founders. The natural range of cynomolgus monkeys spans the mainland of southern Asia, Indonesia, the Philippines, and more recently Mauritius, where a small number of founder animals was imported on a trading ship during the 15th century (Ferguson et al., 2007, Ebeling et al., 2011). Therefore, the cynomolgus monkey is currently the most widely used nonhuman primate species used for drug PK, PD, and safety testing at pharmaceutical companies.

Over the last decade, the use of cynomolgus monkeys as a surrogate model for transporter-mediated DDI studies has been under intense investigations because it is presumed that monkey is the most relevant animal species in which the transport of a drug candidate can be studied, with results extrapolatable to humans. Investigators evaluated how cynomolgus monkeys compare to humans in terms of drug transporter composition, amino acid sequence, tissue expression, substrate specificity, inhibitor potency, and substrate-inhibitor interaction. It is generally presumed that in vivo approaches using monkeys reflect complex, integrated, and dynamic processes in humans and can shed mechanistic insight into drug absorption and disposition beyond what are offered using in vitro models. These animal models can bridge the knowledge gap and enable the extrapolation of in vitro data to clinical outcomes (Figure 1). Furthermore, monkeys have an advantage due to the availability of tissue samples, enabling the measurement of tissue drug concentrations and transporter expression. Bile duct cannulated (BDC) monkeys provide a useful tool to examine biliary excretion. In addition, the recovery of the parent drug in urine can support the determination of renal clearance (CL_r). These methods yield information regarding the excretion processes that transporters are heavily involved in. Determination of systemic, renal, biliary, and tissue clearance can be combined with a transporter modulator to ask a specific transporter-related question. As discussed in the following sections, there are examples of published reports that deployed rifampin and cyclosporin A to inhibit liver organic anion transporting polypeptide (OATP) 1B1 and OATP1B3 in vivo (Shen et al., 2013, Chu et al., 2015, Thakare et al., 2017, Ufuk et al., 2018, Gu et al., 2020, Ogawa et al., 2020a, Eng et al., 2021). Additionally, probenecid, pyrimethamine, elacridar, and curcumin are often co-administered to determine the effects on the inhibition of cynomolgus monkey renal organic anion transporters (OAT) 1 and OAT3 (Tahara et al., 2005, Tahara et al., 2006, Kosa et

al., 2018, Shen et al., 2018b), organic cation transporter (OCT) 2 and multidrug and toxin extrusion (MATE) 1 and MATE2-K (Shen et al., 2016b), as well as P-glycoprotein (P-gp) and breast cancer resistance protein (BCRP), respectively (Karibe et al., 2015, Karibe et al., 2018, Kosa et al., 2018). Furthermore, monkeys share great similarities with humans in terms of the nuclear receptors that regulate transporter expression such as the pregnane X receptor (PXR) (Kim et al., 2010). Not surprisingly, rifampin has been used as a PXR agonist in monkey transporter induction research (Niu et al., 2019, Zhang et al., 2020a). Besides in vivo inhibition, the cynomolgus monkey transporter tool kit has expanded to include individual transporter transfected cell lines, recombinant transporter membrane vesicles, primary cells, and sandwich cultures of monkey hepatocytes, as well as in vivo drug probes, endogenous biomarkers, and inhibitors. Such reagents and models can facilitate drug transporter research. There are also examples of publications describing the use of cynomolgus monkey data for rationalizing the scaling factors used in physiologically-based pharmacokinetic (PBPK) models (Shida et al., 2015, Morse et al., 2017, Liang and Lai, 2021). Based on such collective data, it can be concluded that considerable advancements have been made characterizing and validating cynomolgus monkey transporter models. Moreover, it is apparent that the cynomolgus monkey is valuable in supporting transporter DDI assessment.

(B) Cynomolgus Monkey Shares a High Degree of Isoform Composition, and Amino Acid Sequence Homology with their Human Orthologs

Compared with mice, rats, or dogs, cynomolgus monkeys have a closer evolutionary relationship to humans. They exhibit greater isoform composition and amino acid sequence homology of transporters than other commonly used nonclinical species. A cornerstone of nonhuman primate research with high impact for drug testing was the publication of the draft

whole-genome of the cynomolgus monkey, *Macaca fascicularis*, using the shotgun sequencing approach in 2011 (Ebeling et al., 2011). The main objective of this multicenter investigation was to improve the predictive power of the nonhuman primate models for humans. This investigation mainly focused on identifying 17,387 orthologs of human protein-coding genes in the cynomolgus monkey draft genome. Additionally, this genome facilitates the use of cynomolgus monkeys as a surrogate model for evaluating drug metabolism and conducting transport phenotyping. For example, novel 18 cynomolgus monkey cytochrome P450 (CYP) enzymes were identified in the genome sequence of cynomolgus monkeys, and their amino acid sequences identical to human orthologs were between 94% and 99% (Ebeling et al., 2011).

As expected, cynomolgus monkey exhibits excellent agreement with the human in transporter protein sequence homology (Table 2). Major cynomolgus monkey drug transporter genes of the *SLCO*, *ABCB*, *ABCC*, *ABCG*, *SLC22A*, and *SLC47A* subfamilies have been cloned by different groups recently. They include OATP1B1, OATP1B3, OATP2B1, P-gp, multidrug resistance-associated protein 2 (MRP2), BCRP, OCT1, OCT2, OAT1, OAT2, OAT3, MATE1, and MATE2-K (Tahara et al., 2005, Yasunaga et al., 2008, Shen et al., 2015, Shen et al., 2016b, Kosa et al., 2018). These drug transporters in monkeys display a high degree of similarity (92 to 97%) in amino acid sequences with their human counterparts (Table 2). For example, we cloned the cDNAs of cynomolgus monkey OATP1B1, OATP1B3, and OATP2B1 using the reverse transcription-polymerase chain reaction (RT-PCR) approach with primers derived from the human genes (Shen et al., 2013). The OATP1B1, OATP1B3 and OATP2B1 transporter amino acid sequences between cynomolgus monkeys and humans were 91.9%, 93.5%, and 96.9% identical, respectively (Shen et al., 2013). In contrast, the mouse, rat and dog transporters showed poorer homology compared with humans, ranging from 60% to 70% (Table 2). More

DMD Fast Forward. Published on December 10, 2021 as DOI: 10.1124/dmd.121.000695
This article has not been copyedited and formatted. The final version may differ from this version.

importantly, OATP1B subfamily consists of two highly conserved proteins in both humans and cynomolgus monkeys but not in other species. OATP1B1 and OATP1B3 recognize acidic drugs such as statins as substrates. In contrast, Oatp1b2 and Oatp1b4 are the only orthologue in rodents and dogs, respectively (Hagenbuch and Gui, 2008, Gui and Hagenbuch, 2010). Murine Oatp1b2 and canine Oatp1b4 show 64% and 69% identity of amino acid sequence compared with human OATP1B1, respectively (Table 2). Moreover, while the orthologue to human MATE2-K transcript (NM_001099646) was identified in cynomolgus monkeys (Shen et al., 2016b), no human MATE2-K counterpart has been identified in rodents (Table 2). Identification of the cynomolgus monkey organic cation transporter sequences demonstrate that these mRNAs show very high sequence identities between cynomolgus monkeys and humans, with 99.5%, 99.8%, and 99.6% for OCT2, MATE1, and MATE2-K, respectively (Table 2) (Shen et al., 2016b). Additionally, a high degree of similarity in amino acid sequences was observed in a cynomolgus monkey OAT1 and OAT/3 model, i.e. 97% and 96% identical to human OAT1 and OAT3, respectively (Tahara et al., 2005). Similar profiles (92% to 97% sequence homology, Table 2) were documented in a cynomolgus monkey efflux transporter model for P-gp (Kosa et al., 2018), BCRP (Kosa et al., 2018), MRP2 (Yasunaga et al., 2008), OCT1 (in house data), and OAT2 (in house data). In conclusion, the orthologous transporter proteins are extremely similar, with the amino acid sequence of the major drug transporter proteins commonly differing by less than 10% between humans and cynomolgus monkeys.

(C) Cynomolgus Monkey Transporter Expression Compared with Humans

Transporter activity for a drug is determined by drug affinity and transporter abundance (or expression). Differences in the transporter activity between species can be due to differences in drug affinity and/or transporter expression. Therefore, understanding transporter expression in

cynomolgus monkeys and the difference vs. humans is a prerequisite to extrapolate monkey data to humans.

Over the years, knowledge on cross-species analysis of transport protein expression has increased. Major studies of interspecies similarities and differences in the transporter expression have been compared by quantifying the expression of transporter messenger RNA (mRNA) and protein using reverse transcriptase-polymerase chain reaction (RT-PCR) and immunoblotting, respectively. However, the mRNA expression of transporters is not always correlated with protein abundance of transporters, in particular OATP1B1 and OATP1B3 proteins (Ohtsuki et al., 2012, Prasad et al., 2013, Couto et al., 2020). Furthermore, immunoblotting, an antibody-based quantification assay, has the disadvantage that the resultant band intensities depend on the antibody binding affinity. As a result, it does not allow the comparison of the transporter expression across species due to different antibody binding affinities and lack of cross-species standards (Li et al., 2009b, Hammer et al., 2021). Recent protein quantification by liquid chromatography–tandem mass spectrometry (LC-MS/MS), has revealed interspecies differences in the absolute abundance of transporters of the liver, kidney, and other tissues in humans, cynomolgus monkeys, beagle dogs, and Sprague-Dawley rats (Figure 2) (Li et al., 2009a, Li et al., 2009b, Qiu et al., 2013, Wang et al., 2015, Nakamura et al., 2016, Hammer et al., 2021, Morse et al., 2021). In addition, the expression of various hepatobiliary transporters in cryopreserved hepatocytes is similar to those of the liver tissue. Cross-species comparison by proteomics of the liver indicates that the absolute protein abundance of the transporters of preclinical species is generally greater than that of humans (Figure 2A). While species difference may exist, the monkey is most similar to human in terms of transporter abundance. Takahashi et al. determined the cross-species expression of efflux transporters in the liver and intestine by

DMD Fast Forward. Published on December 10, 2021 as DOI: 10.1124/dmd.121.000695
This article has not been copyedited and formatted. The final version may differ from this version.

real-time RT-PCR using glyceraldehyde 3-phosphate dehydrogenase as an endogenous calibration gene (Takahashi et al., 2008). The expression levels of mRNA of P-gp, BCRP, and multidrug resistance-associated protein 2 (MRP2) were significantly higher in cynomolgus monkeys than those in humans. Among hepatobiliary transporters, OATPs are the most abundant transporter across species. The absolute protein abundance of OATPs in the liver tissue of cynomolgus monkeys and dogs has been determined to be 5.7- and 3.3-fold higher than that of humans (27.4 and 15.7 versus 4.8 fmol/μg membrane protein) (Wang et al., 2015). The next most abundant hepatobiliary transporter in humans and cynomolgus monkeys was OCT1, accounting for 32% and 27% of the total abundance of transporters expressed in cynomolgus monkey and human liver, respectively, whereas Mrp2 and Na^+-taurocholate co-transporting polypeptide (Ntcp) in dogs and rats, respectively, and Oct1 accounted for only 2% of total hepatobiliary transporters in the liver of dogs (Figure 2A) (Wang et al., 2015, Morse et al., 2021). Li et al. reported that the amount of Mrp2 protein in the monkey liver was comparable to that in humans but was approximately 10-fold lower than that in rats (Li et al., 2009b). The abundance of BCRP protein in liver tissues among species was ranked in an order of dog > rat > monkey ≈ human (Li et al., 2009a). But BCRP has been detected in the liver tissue from humans and dogs but not from monkeys and rats in a different study (Wang et al., 2015). Similarly, the hepatobiliary OATP2B1 protein level of cynomolgus monkeys is less than that of humans (0.30 ± 0.10 versus 1.7 ± 0.6 fmol/μg membrane protein) (Wang et al., 2015).

Basit et al. (2019) analyzed cross-species kidney cortical transporter protein abundances in mice, rats, dogs, monkeys, and humans using a targeted proteomics approach (Basit et al., 2019). Generally, higher protein expression of all 19 transporters was found in nonclinical species compared to humans except for P-gp, OCT3, and organic cation / carnitine transporter 1

DMD Fast Forward. Published on December 10, 2021 as DOI: 10.1124/dmd.121.000695
This article has not been copyedited and formatted. The final version may differ from this version.

(OCTN1) (Figure 2B). However, in cynomolgus monkeys, the total abundance of 12 transporters for which proteomics data were available was approximately 3-fold compared with that in humans (Basit et al., 2019). For example, the abundance of human P-gp was similar to that of monkeys, dogs, and rats but it was 2.5-fold higher than mouse P-gp. Some of these transporters, such as OAT1, OAT3, OCT2, MATE1, and P-gp, are clinically relevant. Furthermore, the Chu et al

of distribution of these transporters was identical in both cynomolgus monkeys and humans (Figure 2B) (Basit et al., 2019). These results suggest that cynomolgus monkeys may be a suitable model to support renal transporter research and serve as an in vivo bridge to humans.

Despite an increase in literature data, important knowledge gaps are identified while compiling these proteomics data. One of the reasons is the scarcity of tissue, especially human tissues. Transporter protein expression data in the gastrointestinal tract and brain are limited (Drozdzik et al., 2014, Harwood et al., 2015, Akazawa et al., 2018, Billington et al., 2019, Harwood et al., 2019, Storelli et al., 2021). The absolute abundance of transporter and UDP-glucuronosyltransferase (UGT) proteins in the small intestine of cynomolgus monkeys were determined by using LC/MS and were then compared to the corresponding levels in humans (Akazawa et al., 2018). The expression levels of P-gp and BCRP in the jejunum and ileum in monkeys has been determined to be comparable to that of humans. Of note, BCRP displays the most abundant expression among apical drug efflux transporters in monkeys and humans (Akazawa et al., 2018). Ito et al. measured the absolute abundance of P-gp and other drug transporter proteins at the BBB of cynomolgus monkeys using targeted proteomics (Ito et al., 2011). They discovered that the expression of the various transporters examined in cynomolgus monkeys was similar to those reported for humans in an earlier study (Uchida et al., 2011). For

DMD Fast Forward. Published on December 10, 2021 as DOI: 10.1124/dmd.121.000695
This article has not been copyedited and formatted. The final version may differ from this version.

example, a 1.3-fold difference in the P-gp protein expression at the BBB between monkeys and humans was observed. In contrast, the expression level of P-gp in humans was 2.3-fold smaller than that in mice (Uchida et al., 2011). Pronounced species differences were observed in the brain concentrations and brain-to-plasma concentration ratios of [^{11}C]verapamul, [^{18}F]altanserin, and [^{11}C]GR205171, known P-gp substrates, with higher brain distribution in humans and monkeys than in rats and guinea pigs (Syvanen et al., 2009). It is arguable whether a rat model is a suitable nonclinical model for the prediction of drug brain distribution in humans. Additionally, proteomics-based extrapolation from the in vitro transporter data to the in vivo brain distribution was established for P-gp substrates in cynomolgus monkeys (Uchida et al., 2014).

(D) Cynomolgus Monkey Transporters Display Similar Transport Kinetics and Inhibition Potency Compared to the Corresponding Human Forms

To allow for a meaningful translation of results from cynomolgus monkey studies to clinical outcomes, it is, therefore, of utmost importance to know about the specific transport properties of cynomolgus monkeys compared with humans in terms of transport kinetics and inhibition potency. Recently, the kinetics of cynomolgus monkey transporters has been increasingly evaluated using transfected cell lines and hepatocytes. For example, Shen et al. evaluated substrate specificity between cynomolgus monkey and human hepatic OATP transporters using stably transfected human embryonic kidney (HEK) 293 cells that individually overexpress cynomolgus monkey and human OATP1B1, OATP1B3, and OATP2B1 (Shen et al., 2013). It was revealed that cynomolgus monkey and human hepatic OATPs were qualitatively similar in terms of transport rates of the three chosen substrates [estradiol-17β-glucuronide (E17βG), cholecystokinin-8 (CCK-8), and estrone-3-sulfate E3S)]. Subsequently, the uptake of three human OATP1B1 and OATP1B3 substrates (pitavastatin, pravastatin and rosuvastatin) and

one selective OATP1B3 substrate (telmisartan) was investigated using transfected cell lines (Takahashi et al., 2019). Pitavastatin, pravastatin, and rosuvastatin were demonstrated to be substrates of monkey OATP1B1 and OATP1B3, and telmisartan was suggested to be a substrate of monkey OATP1B3, in a manner similar to human OATP1B. Good agreement between the transport of prototypical substrates by cynomolgus monkey and human OATP1B transporters was observed by other laboratories (Chu et al., 2015, Takahashi et al., 2016). Two studies in both cynomolgus monkey and human hepatocytes investigated the uptake of 9 and 16 OATP1B substrates, respectively (De Bruyn et al., 2018, Eng et al., 2021). Total uptake clearance and passive diffusion were determined in vitro from initial uptake rates in the absence and presence of the OATP inhibitor rifamycin SV. The study suggested that total uptake clearance values in hepatocytes ranged over three orders of magnitude in both species, with a similar rank order and good agreement in the relative contribution of active transport to the total uptake between cynomolgus monkeys and humans. Similar findings were reported by several groups (Shen et al., 2013, Ufuk et al., 2018), who observed comparable Michaelis-Menten constant (K_m) values of OATP1B substrates in hepatocytes between cynomolgus monkeys and humans (Table 3).

To explore the substrate specificity between monkey and human renal organic Cation transporters, cynomolgus monkey OCT2, MATE1 and MATE2-K were independently expressed in HEK-293 cells (Shen et al., 2016b). Based on the results obtained with the six chosen substrates and non-substrates (metformin, 1-methyl-4-phenylpyridinium, tetraethylammonium, cimetidine, estrone-3-sulfate, and methotrexate), it is concluded that cynomolgus monkey and human hepatic organic cation transporters are qualitatively similar. In addition, the pH-dependence experiments were performed with the buffer at any pH between 5 and 11. The transport of metformin mediated by the monkey and human MATE1 was comparable at various

DMD Fast Forward. Published on December 10, 2021 as DOI: 10.1124/dmd.121.000695
This article has not been copyedited and formatted. The final version may differ from this version.

extracellular pH values. Both cynomolgus monkey and human MATE1-mediated uptake increased with increasing extracellular pH, reaching a maximum of pH 9, and decreased when pH was raised from 9 to 11 (Shen et al., 2016b). MATE2-K-mediated metformin uptake also demonstrated comparable pH dependence between monkeys and humans. In contrast, both monkey OCT2- and human OCT2-mediated uptake appeared considerably less sensitive to the increase of pH. Furthermore, available published cross-species K_m values for 20 transporter substrates, such as rosuvastatin (OATP1B1, OATP1B3, OATP2B1, and NTCP) (Shen et al., 2013, Shen et al., 2015, Ufuk et al., 2018, Takahashi et al., 2019), *p*-aminohippurate (OAT1), benzylpenicillin (OAT3) (Tahara et al., 2005, Tahara et al., 2006), and metformin (OCT2, MATE1, and MATE2-K) (Shen et al., 2016b), showed good agreement within a 3-fold difference between cynomolgus monkey and human transporters (Table 3 and Figure 3A).

Inhibitor potency between monkey and human drug transporters has also been compared using single transfected SLC in HEK-293 cells or using membrane vesicles expressing ABC transporters. For example, more than twenty known transporter inhibitors were chosen, which rendered a wide range of half-maximal inhibitory concentration (IC_{50}) values (Table 4) (Shen et al., 2013, Takahashi et al., 2013, Chu et al., 2015, Shen et al., 2015, Shen et al., 2016b, Takahashi et al., 2016, Kosa et al., 2018, Zhang et al., 2019). All except for a few compounds inhibited both cynomolgus monkey and human transporters almost equally, and their IC_{50}s were in good agreement for each transporter (less than 3-fold difference) (Figure 3B). For example, imipramine was a less potent inhibitor of monkey OCT2 than human OCT2 (IC_{50} of 12.3 and 2.1 μM, respectively) (Shen et al., 2016b). Rifampin was a less potent inhibitor of monkey BCRP compared to human BCRP (IC_{50} of 79 and 14 μM, respectively) (Kosa et al., 2018), but KO143 is a more potent monkey BCRP inhibitor than human BCRP (IC_{50} of 0.19 and 1 μM,

respectively). Taken together, these results suggest that cynomolgus monkey transporters often present transport characteristics similar to those of human transporters.

(E) Effects of In Vivo Inhibitors on Transporter Drug Probe PK in Cynomolgus Monkeys

To extend our findings from in vitro to in vivo, many transporter substrate-inhibitor pairs were chosen to be investigated as transporter-mediated DDIs in cynomolgus monkeys. The in vitro transport parameters (K_m and IC_{50}) generated with cynomolgus monkey transporters and primary hepatocytes were comparable to those derived from human transporters and primary hepatocytes (Tables 3 and 4). Consistently, the mean area under plasma concentration-time curve (AUC) values of drug and endogenous probes in cynomolgus monkeys generally increased to a similar extent following coadministration of a reference inhibitor compared to those in humans despite differences in the dose and route of administration (Table 5 and Figure 4). Collectively, these results demonstrate the human relevance of studying the transporter-mediated DDIs in monkeys both in vitro and in vivo (Tahara et al., 2006, Shen et al., 2013, Takahashi et al., 2013, Chu et al., 2015, Shen et al., 2015, Shen et al., 2016a, Shen et al., 2016b, Thakare et al., 2017, Karibe et al., 2018, Kosa et al., 2018, Shen et al., 2018b, Ufuk et al., 2018, Zhang et al., 2019, Gu et al., 2020, Wiebe et al., 2020, Cheng et al., 2021, Eng et al., 2021).

It is important to note that the PK profiles of hepatic OATP1B substrates, including rosuvastatin (Shen et al., 2013, Shen et al., 2015), pitavastatin (Takahashi et al., 2013, Kosa et al., 2018, Ufuk et al., 2018, Eng et al., 2021), atorvastatin (Chu et al., 2015), coproporphyins (CPs) (Shen et al., 2016a, Takehara et al., 2019, Gu et al., 2020), and bile acids as well as their conjugates (Chu et al., 2015, Thakare et al., 2017), have been extensively characterized after coadministration of a single dose of rifampin and cyclosporin A, known OATP inhibitors, in cynomolgus monkeys. In this instance, the AUCs of OATP1B substrates were significantly

altered because of the OATP1B transporter inhibition. In general, these changes were in agreement with reported clinical DDIs (Figure 4). However, Chu et al. demonstrated that the atorvastatin AUC change following rifampin administration in monkeys is 1.5-fold (Chu et al., 2015). Such an AUC ratio is lower than that reported in the clinical studies (5- to 7-fold) described by Lau et al. (Lau et al., 2007) and He et al. (He et al., 2009). On the other hand, a single dose of 20 to 30 mg/kg rifampicin or 75 mg/kg cyclosporin A increased the AUCs of pitavastatin and rosuvastatin by approximately 10- to 39-fold in discrete and cassette DDI studies (Takahashi et al., 2013, Kosa et al., 2018), demonstrating stronger DDI compared to clinical studies (Lai et al., 2016). These results suggest that there is a variability in transporter-mediated statin DDIs in cynomolgus monkeys. Additionally, it might be more difficult to make interpret the data when probe drugs are evaluated in cassette PK study.

In vivo studies documented that probenecid treatment resulted in decreased CL_r and increased AUC of furosemide (OAT1 and OAT3 substrate) and famotidine (OAT3 substrate) in cynomolgus monkeys, as compared to control animals (2.0- to 4.1-fold) (Tahara et al., 2006, Thakare et al., 2017, Shen et al., 2018b). These findings could be explained by the renal transporter OAT1 and/or OAT3 inhibition by probenecid. In contrast, the systemic exposure and renal clearance CL_r of cimetidine, a substrate of renal organic cation transporters, were not affected by probenecid in monkeys (Tahara et al., 2006). These results are in line with the clinical studies (Gisclon et al., 1989, Inotsume et al., 1990, Shen et al., 2019a). While monkey OAT1 and OAT3 shared greatly similar transport characteristics with human orthologs and exhibited suitability in assessing OAT1/3-mediated DDIs in humans, the clinical DDI between famotidine and probenecid could not be reproduced in rats since the Oat3 transport activity and Oct1 expression in the rodent kidney are different to those of humans (Tahara et al., 2006).

There is also emerging evidence that cynomolgus monkeys are considered suitable models for predicting human DDIs involving renal organic cation transporters including OCT2, MATE1, and MATE2-K (Shen et al., 2016b). Consistent with the in vitro inhibition of OCT2-, MATE1-, and MATE2-K-mediated transport of metformin by pyrimethamine, intravenous pretreatment of monkeys with pyrimethamine, a known inhibitor of renal organic cation transporters, decreased the CL_r and increased the AUC of metformin by approximately 50% and 123%, respectively (Shen et al., 2016b), which is in agreement with the clinical DDI data (Weidekamm et al., 1982).

The impact of P-gp and BCRP on drug disposition has been well characterized due to the availability of P-gp and BCRP knockout mice and rats. However, loss of P-gp or Bcrp mRNA and protein expression in the transporter deficient animals may lead to compensatory changes in the expression of other genes involved in drug metabolism and disposition. Additionally, the expression and transporter activity of P-g and Bcrp in rodents may be different from those of humans. Therefore, the potential for misestimating the influence of P-gp and Bcrp knockout mice and rats cannot be ruled out. For example, characterization of P-gp (Mdr1a) and Bcrp knockout rats, using paclitaxel and sulfasalazine as a corresponding probe of P-gp and BCRP, showed that the AUCs of paclitaxel and sulfasalazine were increased by 8-5- and 23.3-fold in comparison with wild-type animals, respectively (Zamek-Gliszczynski et al., 2012). These changes are greater than the magnitudes of DDIs observed in the clinic. Some have resorted to using specific P-gp and BCRP drug substrates and inhibitors in cynomolgus monkey transporter models. Towards this end, investigators have employed P-gp and BCRP inhibitors such as elacridar and curcumin. While elacridar is a dual inhibitor of monkey P-gp and BCRP, curcumin is thought to be a more selective BCRP inhibitor owing to its low affinity for CYP enzymes and

other transporters such as P-gp and MRP2 (Karibe et al., 2018, Kosa et al., 2018). Karibe et al. evaluated if Bcrp knockout mice and BCRP inhibitor-treated cynomolgus monkeys can be used as an animal model to assess the clinical BCRP-mediated DDI (Karibe et al., 2015). The deletion of the Bcrp gene resulted in marked effects on sulfasalazine with a 150-fold increase of AUC following oral administration of sulfasalazine in Bcrp knockout mice compared with wildtype controls. In contrast, curcumin, a potent BCRP inhibitor, increased the AUC of sulfasalazine 2.0- and 3.2-fold at a micro-dose and the therapeutic dose in humans (Kusuhara et al., 2012). The bioavailability changes in mice, which corrected the effect of systemic clearance by Bcrp knockout, correlated better with the AUC changes in humans (i.e., 8.4-fold vs. 2.2- to 3.2-fold). Curcumin increased the AUC of sulfasalazine in cynomolgus monkeys by 6.1-fold (Karibe et al., 2015). Similar increases of sulfasalazine AUC were observed in cynomolgus monkeys when administrated with BCRP inhibitors (i.e., 2.9- to 3.2-fold) (Karibe et al., 2018, Kosa et al., 2018). Overall, these results support the utility of cynomolgus monkeys as a surrogate model that could enable DDI risk assessment before advancing a new molecular entity (NME) to the development stage, as well as providing mechanistic insights regarding transporter-mediated DDI.

DMD Fast Forward. Published on December 10, 2021 as DOI: 10.1124/dmd.121.000695
This article has not been copyedited and formatted. The final version may differ from this version.

APPLICATION OF CYNOMOLGUS MONKEY TRANSPORTER MODELS

(A) Assessment of Transporter-Mediated DDI Risk for NMEs

Because cynomolgus monkeys exhibited comparable transport characteristics and the known human transporter DDIs are recapitulated in the cynomolgus monkey as described above, cynomolgus monkeys serve as an appropriate model for predicting human DDIs involving transporters. Several studies have documented that cynomolgus monkey has been used for preclinical assessment of transporter DDIs with NMEs as test perpetrators. Ogawa et al. recently investigated a transporter-mediated DDI using an in vitro cell system and in vivo cynomolgus monkey model (Ogawa et al., 2020a, Ogawa et al., 2020b). Oral admiration of either rifampicin or cyclosporine A significantly increased the AUC of intravenously administered pemafibrate, a drug recently approved by Japanese Pharmaceuticals and Medical Devices Agency (PMDA), by 7.4- and 4.9- fold, respectively, in cynomolgus monkeys. In agreement with this, clinical studies with pemafibrate showed that rifampicin (600 mg) and cyclosporine (600 mg) increased the AUC of pemafibrate by 11- and 14-fold, respectively (Pemafibrate; Japanese prescribing information 2018; http://www.pmda.go.jp/). These results suggested that pemafibrate was actively taken up by hepatocytes via OATP1B and cleared from plasma similarly in cynomolgus monkeys and humans.

The second example involves a drug candidate in discovery and early development. During the routine DDI risk assessment screening of transporter DDIs risk in drug discovery, it was determined that a Bristol Myers Squibb (BMS) compound was a potent inhibitor of OATP1B1 and OATP1B3 with the IC_{50} of 0.24 and 0.65 μM, respectively. An IVIVE analysis using the mechanistic static model indicated a ratio of the victim AUC in the presence and absence of perpetrators (R-value) of 1.4, which suggests a potential to impede the uptake of

OATP1B substrates into hepatocytes from the portal circulation. Because the OATP1B DDI prediction with a static model is conservative and the binding of the BMS compound to serum proteins is high (99.8% and 99.6% in human and monkey, respectively), a pharmacokinetic DDI study was performed to determine if there is any DDI in monkeys. Oral DDI studies in cynomolgus monkeys were performed at two perpetrator doses to evaluate the potential for interactions between the known OATP1B substrate rosuvastatin and the compound. The two perpetrator doses for the BMS compound were necessary due to a difference in the elimination pathways of the compound between monkeys and humans as well as the difference in the hepatic blood flow between the two species. When the oral dose of the compound for the monkey DDI was selected based on achieving similar systemic concentrations in monkeys as in humans, a marked DDI was observed (11-fold increase in the AUC of rosuvastatin). However, when the dose for the DDI was chosen based on achieving similar portal vein concentrations in monkeys as in humans, only a moderate interaction was seen (2.2-fold increase in the AUC of rosuvastatin). The above-described monkey analysis subsequently triggered in vivo clinical DDI evaluations. The clinical DDI study using rosuvastatin as an OATP1B probe showed that the extent of the plasma AUC increases in the human DDI study was comparable to that in the monkey DDI study in which the dose was selected based on achieving similar portal vein concentrations in monkeys as in humans at a therapeutically relevant dose. These investigations suggest that the cynomolgus monkey has utility in predicting OATP-mediated DDIs in the clinic, with the need of careful selection on perpetrator doses.

The third example using the cynomolgus monkey for the DDI evaluation was on OAT1/3 inhibition. With the goal of predicting a human DDI, Ball et al. (2017) studied the extent of interaction between S44121 as victim and probenecid as an inhibitor of OAT1 and OAT3

because the monkey has previously been reported to be a good preclinical model for renal organic anion transporter inhibition (Ball et al., 2017). The S44121 AUC ratios in monkeys were between 3.0 and 3.5, which was slightly higher than the clinical observations (2.2). Additionally, an AUC ratio of 1.6 was predicted for S44121 in the presence of probenecid using a PBPK model, which was slightly smaller than the results obtained from the clinical DDI study. However, it is worth noting that the elimination pathway of S44121 in cynomolgus monkeys is different than in humans (Ball et al., 2017), which may explain the over-prediction in monkeys.

(B) Prediction of Clearance Involving Transporters

Cynomolgus monkey has been evaluated as a preclinical model to predict OATP1B-mediated clearance by assessing IVIVE and applying cross-species extrapolation because of the excellent agreement with humans in OATP1B protein sequence homology and transport activity (Kimoto et al., 2017, De Bruyn et al., 2018, Matsunaga et al., 2019, Liang et al., 2020, Eng et al., 2021). Such studies would increase confidence in the subsequent extrapolation of human in vitro transporter-mediated uptake to clinical hepatic clearance. De Bruyn et al. recently demonstrated the utility of this preclinical model to delineate drug hepatic uptake and predict human in vivo intrinsic hepatic clearance (De Bruyn et al., 2018). The uptake of 9 OATP1B drug substrates: bosentan, cerivastatin, fexofenadine, repaglinide, rosuvastatin, pitavastatin, pravastatin, telmisartan, and valsartan in cynomolgus monkey and human hepatocytes were evaluated. The in vitro uptake parameters including total and active uptake clearance, passive diffusion, the contribution of active transport to total uptake in hepatocytes, and in vitro intracellular binding across a wide range of values, displayed a similar rank order and agreement between cynomolgus monkeys and humans. The in vivo hepatic clearance values of 9 OATP1B drug substrates determined by intravenous pharmacokinetics studies in cynomolgus monkeys

exhibited comparable results to human parameters. In addition, the in vivo monkey and human hepatic clearance values were well predicted by corresponding hepatocyte uptake data with mean 2.7- and 3.8-fold bias, respectively (De Bruyn et al., 2018). Additionally, the application of cross-species empirical scaling factors either as mean or individual drug values improved the prediction of human hepatic clearance from human hepatocyte data. Subsequently, studies were performed with the same drugs in beagle dogs and Sprague Dawley rats by the same group (Matsunaga et al., 2019). Large interspecies differences in hepatocyte-to-medium concentration ratio for total and unbound drug (K_p and $K_{p,uu}$) values were seen with the general rank order of cynomolgus monkey ≈ human < dog < rat for the 9 drugs (Matsunaga et al., 2019). Furthermore, the use of monkey empirical scaling factors for human hepatic clearance prediction resulted in a prediction bias of 3-fold, with about 70% of drugs predicted within 2-fold of the in vivo hepatic clearance values. In contrast, both the prediction accuracy and percentage of drugs within the same error threshold were lower using dog- and rat-specific scalars (Matsunaga et al., 2019). Comparable in vitro uptake clearance and fraction transported by OATP1B between monkey and human hepatocytes were also observed for 16 large lipophilic acid compounds with molecular weight approximately 400 to730 Da, logP 3.5 to8, and acid pKa <6 (Eng et al., 2021). Furthermore, Kimoto et al. evaluated the dose of 6 OATP1B drug substrates excreted in the bile of nonclinical species including cynomolgus monkeys, dogs, and rats (Kimoto et al., 2017). They found that the biliary excretion clearance values determined with BDC monkeys were comparable to those in humans. As a result, the minimal species differences observed for the OATP1B-mediated transport between cynomolgus monkey and human hepatocyte uptake and excretion, both in vitro and in vivo, support the use of cynomolgus monkey as a nonclinical model to predict drug hepatic clearances.

(C) Improvement of Transporter PBPK Modeling

To devise an effective mechanistic IVIVE strategy, the incorporation of transporter-mediated uptake and efflux into a PBPK model is necessary. Consequently, transporter parameters including expression levels and transport kinetics are determined for each process and used in conjunction with system and physiology parameters to predict drug behavior in vivo. When integrating drug-related parameters into a model, the key transport kinetics, including active kinetics, are often described by the K_m and the maximal flux rate (J_{max}). Alternatively, the uptake clearance (CL_{up}), assuming substrate concentrations well below the K_m, can be used. Although significant progress has been made, the application of PBPK for transporter-mediated DDI in drug development is relatively uncommon since the predictive performance of PBPK models for transporter-mediated DDI is not well established compared to CYP-mediated DDI (Taskar et al., 2020). The major challenge of transporter PBPK is that it requires a detailed understanding of the complex role of drug transporters in the organs (e.g., liver, kidney, gut, and brain), transporter-enzyme interplay, and the physiological parameters that define the membrane barriers. For example, a range of physiological factors essential to the gut function can markedly impact drug absorption. These include gastric emptying, intestinal transit time, gastrointestinal pH, fluid dynamics, and intestinal segmental blood flow. In addition, empirical scaling factors are specifically required for in vitro active uptake parameters determined in primary hepatocytes to compare to the in vivo plasma clearance in PBPK modeling efforts when evaluating the prediction of hepatic clearance governed by OATP1B- and OCT1-mediated uptake in nonclinical species and humans (Jones et al., 2012). The ability to include liver drug concentrations for PBPK modeling and estimate in vitro to in vivo prediction of human liver drug accumulation is restricted since human liver partitioning cannot be directly measured. However, a validated

IVIVE of drug liver partitioning in cynomolgus monkeys, through the simultaneous liver and plasma sampling and in vitro monkey hepatocyte uptake, is thought to be a suitable approach for the assessment of liver accumulation (Morse et al., 2015, Morse et al., 2017). For example, Morse et al. assessed the in vitro to in vivo liver partitioning for OATP1B (rosuvastatin and bosentan) and OCT1 substrates (metformin) utilizing ultrasound-guided liver sampling technique in cynomolgus monkeys (Morse et al., 2017). They also incorporated the liver along with plasma data for determination of in vivo transport parameters with PBPK modeling. In turn, the scaling factors obtained from the IVIVE validated from the prediction in cynomolgus monkeys can further be applied for the prediction of human hepatic clearance and assessment of human liver accumulation using in vitro human hepatocyte data (Morse et al., 2017). Such assessments of in vitro to in vivo liver partitioning and incorporation of liver and plasma concentrations for the determination of in vivo transport parameters with PBPK modeling have been expanded to the other OATP1B drug substrates such as bromfenac, carotegrast, and pemafibrate (Ogawa et al., 2019, Cheng et al., 2021). As a result, it is envisioned that the predictability of a PBPK model and the scaling factor for the IVIVE need to be validated with measured monkey liver concentration and/or pharmacokinetic DDI data. A human PBPK model incorporating the in vitro human transporter data and scaling factors obtained from monkey PBPK modeling validation would be valuable in drug discovery and early development (Liang and Lai, 2021).

(D) Identification, Characterization, and Validation of Transporter Endogenous Biomarkers

The last decade has witnessed important efforts toward the identification, characterization, and validation of endogenous transporter biomarkers, with numerous examples of researchers employing the cynomolgus monkey as a model species. While conventional

approaches to assess clinical DDI risk using a probe drug that is concomitantly administered with an investigational drug has limitations such as the safety concerns of specific drug probes, uncertain therapeutically efficacious dose in the early development phase, and often conservative prediction by using FDA and EMA mechanistic static model method, the use of circulating and urinary endogenous biomarkers that are selective for individual or combinations of hepatic and renal transporters may solve the dilemma. Using endogenous biomarkers could circumvent the need to dose substrate drugs and thus reduce pill burden in clinical trials. The biomarker data generated in Phase I studies together with model-based predictions would complement regulatory decision tree-based approaches by minimizing false-positive predictions. Consequently, the investigation of endogenous clinical biomarkers of transporters has increased exponentially in the last few years (Chu et al., 2018, Rodrigues et al., 2018, Mochizuki et al., 2021). In this regard, cynomolgus monkey transporter models have played a pivotal role in the identification and validation of novel transporter endogenous biomarkers.

The suitability of coproporphyrin I (CPI) and CPIII as endogenous biomarkers of OATP1B were initially evaluated in nonclinical studies (Shen et al., 2016a). CPI and CPIII were shown to be substrates of cynomolgus monkey and human OATP1B1 and OATP1B3 using HEK-293 cells overexpressing isoform transporter of monkey or human OATP1B subfamily, as well as monkey and human hepatocytes. Oral administration of 100 mg/kg cyclosporin A increased the AUC of CPI and CPIII by 2.6- and 5.2-fold, respectively, and 15 mg/kg rifampicin increased the AUCs by 2.7- and 3.6-fold, respectively (Shen et al., 2016a). In agreement, the AUC of rosuvastatin, a probe drug, in cynomolgus monkeys increased 6.3- and 2.9-fold by the cyclosporin A and rifampin treatments, respectively, in the same animals (Shen et al., 2013, Shen et al., 2015). Furthermore, in South Asian Indian, black, white, and Hispanic subjects,

administration with 600 mg rifampin orally increased the AUC of CPI and CPIII by 2.4- to 3.7-fold, respectively, indicating similar CP changes between cynomolgus monkeys and humans (Figure 4 and Table 5) (Lai et al., 2016, Shen et al., 2018a). The absorption and disposition of CPI in cynomolgus monkeys following oral and intravenous administration of CPI-d8 were further examined (Gu et al., 2020). CPI-d8 showed low absolute oral bioavailability (i.e. 3.2%), implying limited intestinal absorption and enterohepatic circulation of CPI as it is metabolically stable (Gu et al., 2020). Consistently, a BDC monkey study indicated that CPI and CPIII did not undergo significant enterohepatic circulation as the plasma CP concentrations were not altered in BDC monkeys compared with normal animals (Takehara et al., 2019). Additionally, by leveraging the cynomolgus monkey data, Thakare et al. were able to identify 5 bile acid 3-O-sulfate conjugates as novel endogenous biomarker candidates for OATP1B (Thakare et al., 2017). These biomarker candidates were then validated in clinical studies (Takehara et al., 2018, Mori et al., 2020). Furthermore, Chu et al. also evaluated cynomolgus monkeys as a translatable model to assess OATP1B-mediated DDI and identified total and unconjugated bilirubin as well as several bile acids as potential endogenous probes of OATP1B inhibition (Chu et al., 2015). Cynomolgus monkeys orally received different doses of cyclosporin A (4, 20, and 100 mg/kg) and rifampin (1, 3, 10, and 30 mg/kg) which yielded dose-dependent increases of the AUC of the biomarker candidates such as CPs and glycochenodeoxycholate-3-sulfate, demonstrating the in vivo sensitivity of the endogenous compounds as probes of OATP1B (Thakare et al., 2017, Gu et al., 2020). These nonclinical studies greatly help identify and evaluate endogenous biomarkers of OATP1B inhibition.

Cynomolgus monkeys have also been utilized to investigate endogenous biomarkers for renal transporters (Shen et al., 2018b). Specifically, cynomolgus monkeys were pretreated with

an intravenous administration of 40 mg/kg probenecid that is an inhibitor of OAT1 and OAT3. The pretreatment increased the AUC of furosemide, a known OAT1 and OAT3 substrate, by 4.1-fold in monkeys. These increases are similar to the changes reported in clinical studies (4.1-fold vs. 3.1- to 3.7-fold) (Smith et al., 1980, Shen et al., 2019a). Additionally, an untargeted metabolomics analysis was applied to plasma samples to screen endogenous compounds that were associated with OAT1 and OAT3 inhibition in monkeys. Plasma concentrations of pyridoxic acid and homovanillic acid concentrations were significantly increased at 1 or 3 hours after probenecid treatments compared with the vehicle-treated animals. Targeted LC-MS/MS analysis further confirmed that the pyridoxic acid and homovanillic acid AUCs were increased by approximately 2- to 3-fold by probenecid pretreatments. A clinical study examined and validated pyridoxic acid as a plasma-based endogenous biomarker of OAT1 and OAT3 in humans (Shen et al., 2019a). Administration of probenecid markedly increased the AUC of pyridoxic acid by 3.1- to 3.2-fold compared with the pre-study and furosemide groups. Transporter phenotyping experiments using singly stable transporter transfected cell lines indicated that pyridoxic acid and homovanillic acid were substrates for human OAT1, OAT3, OAT2 (homovanillic acid), and OAT4 (pyridoxic acid), but not OCT2, MATE1, MATE2K, OATP1B1, OATP1B3, and NTCP (Shen et al., 2018b). Collectively, these results suggest that cynomolgus monkeys are useful in identifying and examining endogenous biomarker candidates for a better understanding of their translational value.

(E) Elucidation of the Mechanism of Complex PK and Toxicity Involving Transporter

Mechanistic understanding of complex drug disposition, DDIs, and toxicity in the clinic, with potential involvement of numerous elimination pathways and diverse enzyme-transporter interplay has been challenging. Using cynomolgus monkey models, Zhang et al., examined in

vivo effects of rifampicin, a potent PXR agonist, on the activity and expression of hepatic OATP1B (Zhang et al., 2020a). The study reported that plasma levels of CPI and CPIII, OATP1B endogenous biomarkers were not changed in monkeys after multiple rifampicin treatments compared to non-treatment conditions and that the expressions of OATP1B1 and OATP1B3 genes were not induced in the liver (0.85-1.3-fold). In contrast, the plasma concentrations of 4β-hydroxycholesterol, a CYP3A endogenous biomarker, were increased by 3.9-fold and the hepatic and intestinal CYP3A8 mRNA levels were markedly increased by multiple treatments of rifampicin in same animals (3.7- to 5.0-fold). These results obtained from the cynomolgus monkey model validate that OATP1B1 and OATP1B3 are not induced by rifampicin in cynomolgus monkeys. These findings provide a better understanding of the clinical results of OATP1B drug substrates such as statins with PXR inducers (Zhang et al., 2020a). This is important since the effect of commonly used inducers on the expression and functional activity of OATP1B is poorly understood and the reports that describe the OATP1B induction as decreased systemic exposure of probe substrates and increased mRNA and protein levels are limited and conflicting. Moreover, there are two major clinical challenges for OATP1B induction investigations. First, the selectivity of OATP1B drug probes is not well established as most statins are substrates of induced CYP enzymes (e.g. CYP3A4) and efflux transporters (e.g. MRP2). Second, it is not practical to include a tissue biopsy procedure in a clinical study protocol although the determination of transporter expression in the gut and liver tissues following treatment with PXR inducers has been considered the most direct way to assess transporter and drug-metabolizing enzyme induction. Zhang et al. evaluated the effect of multiple administration of rifampicin on gene expression of OATP1B1, OATP1B3, and the major drug transporters in cynomolgus monkey liver, small intestine, and kidneys (Zhang et al.,

2020a). OATP1B1 and OATP1B3 mRNA levels in the liver were not altered by the rifampin treatment. These results are in line with an in vitro hepatocyte induction study that showed a minimal change of OATP1B mRNA in cynomolgus monkey and human hepatocytes treated with rifampin (Niu et al., 2019).

Cynomolgus monkeys and primary cultures of monkey renal proximal tubule epithelial cells have been used to evaluate the role of renal transporters in the cytotoxicity of three Pfizer exploratory drug candidates with varying degrees of nephrotoxicity in cynomolgus monkeys (Cai et al., 2009). Compound PF-1 was nephrotoxic in cynomolgus monkeys. Therefore, the nephrotoxicity of PF-1 was qualitatively compared to two other leads PF-2 and PF-3. The severity of kidney toxicity was ranked as PF-2 > PF-1 > PF-3 in monkeys, with PF-2 inducing mortality at all doses and PF-3 eliciting only mild nephrotoxicity in cynomolgus monkeys. The cytotoxicity was then characterized using lactate dehydrogenase release assay in primary cultures of monkey and human renal proximal tubule epithelial cells for comparisons. The rank of cytotoxicity in monkey kidney proximal tubule cells was PF-2 > PF-3 > PF-1 whereas that in human kidney proximal tubule cells is PF-2 > PF-1 > PF-3 (Cai et al., 2009). Transporter phenotyping studies using transporter transfected cell lines indicated that these organic anions were substrates for human OAT1 (PF-1 and PF-3) and OAT3 (PF-1, PF-2, and PF-3). Consequently, pretreatment of cynomolgus monkeys with probenecid increased the AUC of PF-3 by approximately 2-fold compared to untreated monkeys. As a result, OAT1 and/or OAT3 may be responsible for the uptake of these drugs in kidney renal proximal tubule epithelial cells, which directly or indirectly lead to nephrotoxicity in vivo (Cai et al., 2009).

CONSIDERATIONS WHEN TRANSLATING TRANSPORTER DATA FROM CYNOMOGUS MONKEY MODELS TO CLINICAL OUTCOMES WHEN PREDICTING HUMAN PK AND DDI

When we interpret the data of cynomolgus monkey transporter translational research for predicting human PK and DDIs, we emphasize the need to consider the caveats that apply to such research. Species differences in expression and activity of CYP enzymes are observed between monkeys and humans (Uno et al., 2006). For instance, the orthologue of CYP2C76, a functional drug-metabolizing enzyme in the liver of cynomolgus monkeys, is not expressed in humans (Uno et al., 2006, Emoto et al., 2013). The diclofenac 4'-hydroxylation activities in the microsomes derived from monkey liver and small intestine are significantly lower compared with those in human liver and intestinal microsomes (Emoto et al., 2013). In addition, sulfaphenazole strongly inhibits diclofenac 4'-hydroxylation in human liver microsomes whereas it does not inhibit diclofenac 4'-hydroxylation in monkeys. Cynomolgus monkey CYP2C19 has presented higher diclofenac 4'-hydroxylase activity than monkey CYP2C9 even though this reaction is a marker reaction of human CYP2C9 (Emoto et al., 2013). Therefore, it is not uncommon that the species differences between cynomolgus monkey and human transporters are present in tissue expression, substrate specificity, and inhibitor potency. For example, the OATP2B1 protein level was approximately 6-fold greater in the human liver compared with the cynomolgus monkey liver (Wang et al., 2015). Chu et al. evaluated the inhibitory effect of a single dose of rifampin on in vitro transport and PK of rosuvastatin and atorvastatin in cynomolgus monkeys (Chu et al., 2015). While rifampin strongly inhibited the monkey OATP1B1- and OATP1B3-mediated uptake of rosuvastatin and atorvastatin in vitro, different changes in the probe AUC between rosuvastatin and atorvastatin were observed in monkey DDI

studies. In agreement with clinical observations, 18 mg/kg rifampin significantly increased the AUC of intravenously administered rosuvastatin by 3-fold, and increased that of orally administered rosuvastatin by 6-fold, respectively. In contrast to clinical findings, rifampin treatment did not significantly increase plasma exposure of either intravenously or orally administered atorvastatin, suggesting species differences in the elimination pathways and contribution by OATP1B (Chu et al., 2015). Additionally, a DDI study in cynomolgus monkeys was also performed for evaluating the role of OAT1 and OAT3 in the renal secretion of S4412 (Ball et al., 2017). The coadministration of probenecid with S44121 resulted in a 3.2-fold increase in the plasma AUC of S44121 and a 5.1-fold decrease in the renal clearance in cynomolgus monkeys. Although the AUC change in monkeys was in agreement with that in humans (i.e., 3.2- vs. 2.2-fold), there is a species difference in the S44121 elimination between monkeys (mainly hepatic metabolism) and humans (mainly renal excretion of unchanged drug), rendering comparison between the two DDI studies challenging (Ball et al., 2017). Nevertheless, as long as the differences between species are understood (e.g., liver OATP2B1 expression), they can be accounted for when translating monkey data to humans. The differences would be used for mechanism-informed understanding when the monkey model is not applicable. Therefore, understanding the discrepancies related to the monkey and human transport kinetics and inhibition properties, and significantly different PK and disposition properties between species (e.g., achieving equivalent exposure, elimination routes, protein binding, metabolic profiles) could be valuable for cross-species translation.

Although reference inhibitors (e.g. rifampin) and model substrates (e.g. rosuvastatin) have been used in cynomolgus monkey and human DDI studies, caution is needed when using these tools because drugs may have effects on other transporters and/or drug-metabolizing

enzymes and may make interpretation of the results ambiguous (Table 1). For instance, probenecid is a reference inhibitor of renal transporters OAT1 and OAT3. However, it inhibits the in vitro activity of hepatic drug transporters OATP1B1 and OATP1B3 with half-maximal inhibitory concentration (IC_{50}) values of 167 ± 42.0 and 76.0 ± 17.2 μM, respectively, in transporter-overexpressing human embryonic kidney cells. In addition, probenecid significantly inhibited the uptake of coproporphyrins (CPs) and statins, the endogenous and exogenous substrates, in cynomolgus monkey and human hepatocytes (Kosa et al., 2018, Zhang et al., 2020b). Consequently, administration with 1000 mg probenecid alone or in combination with furosemide increased the AUC values of CPI, an endogenous biomarker of OATP1B1 and OATP1B3, by 1.4- and 1.6-fold compared to pre-dose levels. Despite increased systemic exposures, no decreases in CPI CL_R were observed (Zhang et al., 2020b). In line with the endogenous biomarker data, probenecid increased the AUC of OATP1B drug probe rosuvastatin in cynomolgus monkeys and humans by 3.3- and 2.6-fold, respectively (Kosa et al., 2018, Wiebe et al., 2020).

CONCLUSIONS AND PERSPECTIVE

Mounting evidence suggests that cynomolgus monkey models are valuable when dissecting the different functional roles of transporters in drug absorption, distribution, and elimination. In this review, we described the suitability of various cynomolgus monkey models to study major intestinal, hepatic, and renal drug transporters by comparing protein sequence, expression, and function between monkeys and humans. Cynomolgus monkey transporter models are novel tools that allow the generation of in vitro and in vivo data as well as supporting in vitro-to-in vivo translation for predicting drug PK and DDIs. Cynomolgus monkeys together with other preclinical models are the nonclinical species currently being used as models for studying drug transporters, and the research in this area is actively growing.

One of the major weaknesses regarding transporter research in drug discovery and development has been the tendency to oversimplify relevant factors underlying transporter-mediated drug disposition and interactions. Typically, in vitro transport kinetic parameters are obtained in isolated and different systems, thereby ignoring their interrelationships and systems dependencies. These include the use of transfected cell lines and membrane vesicles, and isolated primary cells as well as different culture and experimental conditions, and data analysis methods. Simple decision trees and ratios based on such isolated parameter values are used to assess DDI risks for compounds in discovery and development. In most cases, however, these approaches do not take into account transporter substrate overlap, transporter-transporter interplay, transporter-enzyme interplay, transport saturation, the relevance of in vitro experimental conditions to in vivo, and various interlinked processes between drug dosing and the concentration-time profiles in blood and tissues. In addition, each in vitro assay and system has its advantages and limitations that need careful considerations. For example, it has been reported that there is

considerable variability across laboratories (up to 100-fold)in apparent in vitro P-gp and OATP1B1 IC_{50} values, leading to difficulties in or invalidating the use of mechanistic static models in IVIVE for transporter DDI assessments (Cook et al., 2010, Duan et al., 2017). In addition, a direct scaling of uptake clearance using primary hepatocytes to predict the in vivo clearance typically results in an underprediction, and the scaling factor is compound-dependent (Jones et al., 2012). The underprediction is not completely explained by the loss of transporter expression and activity, although it is possible during hepatocyte isolation, cryopreservation, and storage. In this regard, the use of hepatocyte transport kinetics and uptake clearance data generated in the presence of serum albumin or human plasma may improve IVIVE supporting human clearance prediction (Nozaki and Izumi, 2020). However, such an approach is controversial and needs further validation.

Challenges related to the IVIVE for transport-mediated clearance and DDI predictions may be addressed using cynomolgus monkey transporter models that allow simultaneous and dynamic changes in drug concentrations vs. time in blood, urine, bile, and tissues in which multiple processes, including active transport, passive diffusion, metabolism, and protein binding, are involved. Such models can be used to examine an in vivo DDI, thus bridging the in vitro inhibitory potential to the extent of the in vivo inhibition. The approach requires addressing each experiment and IVIVE caveat, carefully designing the PK study and optimizing experiment conditions, and appropriately selecting and validating model transporter substrates and reference inhibitors. The animal-to-human translation assumes that the PK of probe substrates and inhibitors in monkeys is similar to that in humans. For example, the disposition of rosuvastatin after oral administration of [^{3}H]rosuvastatin (3 mg/kg) to BDC cynomolgus monkeys was evaluated, and the results indicated there was consistency in the elimination pathway of oral

rosuvastatin between cynomolgus monkeys and humans, validating that the monkey can be used as a probe to assess drug inhibition of OATP1B both in vitro and in vivo (Shen et al., 2015). Therefore, the information gathered on transport kinetics and elimination pathways between monkeys and humans for individual drugs is valuable for the development of more streamlined predictive models.

Transporter-mediated DDIs can occur at a tissue level that is not reflected by plasma exposure changes. Tissue-oriented PK studies in cynomolgus monkeys may be useful as surrogate markers for tissue-level DDIs. For example, Cheng et al. documented the changes of liver and systemic exposures of OATP1B substrates, including rosuvastatin, carotegrast, bromfenac, CPI and CPIII, in the presence and absence of OATP inhibitor rifampin in cynomolgus monkeys (Cheng et al., 2021). Rifampin increased the AUC of rosuvastatin, bromfenac, carotegrast, CPI, and CPIII by 2.3-, 2.1-, 9.1-, 5.4-, and 8.8-fold, respectively, However, different changes in liver concentration were observed between the compounds. The liver-to-plasma concentration ratios of rosuvastatin and bromfenac were decreased by rifampin. However, the liver concentration of the drugs remained unchanged. In contrast, the liver concentrations of carotegrast, CPI, and CPIII were increased at 6 h after rifampin dose. The PBPK analysis indicated that the plasma concentrations of OATP1B substrates were predominantly governed by OATP1B-mediated uptake whereas the liver exposures in the presence OATP1B inhibition were regulated by passive diffusion, sinusoidal uptake, metabolism, and cannicular efflux (Cheng et al., 2021).

The major future direction of cynomolgus monkey transporter research is to continue evaluating known human transporter drug substrates and inhibitors in vitro and in vivo. It is important to develop a database of information between in vitro and in vivo, and between

cynomolgus monkeys and humans, to create improved mathematical models, or to make better human predictions from in vitro data alone.

While transporter research in primates can be advocated based on the body of literature to date, it goes without saying that their use should be limited as much as possible and carefully guided by an institution's review board and Animal Care & Use Committee (Burm et al., 2014, Stokes, 2015). As described herein, cynomolgus monkeys present as a useful human surrogate in support of drug transporter research. In many respects, they are superior to humanized rodent models. However, it is worth noting that the ultimate goal will be to minimize animal testing altogether and progress transporter science to a point that alternative tools, such as human PBPK, artificial intelligence, and human organ on a chip, are used in support of NME discovery and development. In the meantime, with the above vision in mind, careful use of monkey models will continue to support validation of IVIVE related to transporter-mediated clearance prediction and DDI.

Authorship Contributions

Participated in research design: NA

Conducted experiments: NA

Contributed new reagents or analytic tools: NA

Performed data analysis: NA

Wrote or contributed to the writing of the manuscript: Shen, Yang, and Rodrigues

Financial Disclosure

No author has an actual or perceived conflict of interest with the contents of this article.

References

Akazawa T, Uchida Y, Miyauchi E, Tachikawa M, Ohtsuki S and Terasaki T (2018) High Expression of UGT1A1/1A6 in Monkey Small Intestine: Comparison of Protein Expression Levels of Cytochromes P450, UDP-Glucuronosyltransferases, and Transporters in Small Intestine of Cynomolgus Monkey and Human. *Mol Pharm* 15: 127-140.

Ball K, Jamier T, Parmentier Y, Denizot C, Mallier A and Chenel M (2017) Prediction of renal transporter-mediated drug-drug interactions for a drug which is an OAT substrate and inhibitor using PBPK modelling. *Eur J Pharm Sci* 106: 122-132.

Basit A, Radi Z, Vaidya VS, Karasu M and Prasad B (2019) Kidney Cortical Transporter Expression across Species Using Quantitative Proteomics. *Drug Metab Dispos* 47: 802-808.

Billington S, Salphati L, Hop C, Chu X, Evers R, Burdette D, Rowbottom C, Lai Y, Xiao G, Humphreys WG, Nguyen TB, Prasad B and Unadkat JD (2019) Interindividual and Regional Variability in Drug Transporter Abundance at the Human Blood-Brain Barrier Measured by Quantitative Targeted Proteomics. *Clin Pharmacol Ther* 106: 228-237.

Burm SM, Prins JB, Langermans J and Bajramovic JJ (2014) Alternative methods for the use of non-human primates in biomedical research. *ALTEX* 31: 520-529.

Cai H, Agrawal AK, Putt DA, Hashim M, Reddy A, Brodfuehrer J, Surendran N and Lash LH (2009) Assessment of the renal toxicity of novel anti-inflammatory compounds using cynomolgus monkey and human kidney cells. *Toxicology* 258: 56-63.

Cheng Y, Liang X, Hao J, Niu C and Lai Y (2021) Application of a PBPK model to elucidate the changes of systemic and liver exposures for rosuvastatin, carotegrast, and bromfenac followed by OATP inhibition in monkeys. *Clin Transl Sci*.

Chu X, Liao M, Shen H, Yoshida K, Zur AA, Arya V, Galetin A, Giacomini KM, Hanna I, Kusuhara H, Lai Y, Rodrigues D, Sugiyama Y, Zamek-Gliszczynski MJ, Zhang L and International Transporter C (2018) Clinical Probes and Endogenous Biomarkers as Substrates for Transporter Drug-Drug Interaction Evaluation: Perspectives From the International Transporter Consortium. *Clin Pharmacol Ther* 104: 836-864.

Chu X, Shih SJ, Shaw R, Hentze H, Chan GH, Owens K, Wang S, Cai X, Newton D, Castro-Perez J, Salituro G, Palamanda J, Fernandis A, Ng CK, Liaw A, Savage MJ and Evers R (2015) Evaluation of cynomolgus monkeys for the identification of endogenous biomarkers for hepatic transporter inhibition and as a translatable model to predict pharmacokinetic interactions with statins in humans. *Drug Metab Dispos* 43: 851-863.

Cook JA, Feng B, Fenner KS, Kempshall S, Liu R, Rotter C, Smith DA, Troutman MD, Ullah M and Lee CA (2010) Refining the in vitro and in vivo critical parameters for P-glycoprotein, [I]/IC50 and [I2]/IC50, that allow for the exclusion of drug candidates from clinical digoxin interaction studies. *Mol Pharm* 7: 398-411.

Couto N, Al-Majdoub ZM, Gibson S, Davies PJ, Achour B, Harwood MD, Carlson G, Barber J, Rostami-Hodjegan A and Warhurst G (2020) Quantitative Proteomics of Clinically Relevant Drug-Metabolizing Enzymes and Drug Transporters and Their Intercorrelations in the Human Small Intestine. *Drug Metab Dispos* 48: 245-254.

De Bruyn T, Ufuk A, Cantrill C, Kosa RE, Bi YA, Niosi M, Modi S, Rodrigues AD, Tremaine LM, Varma MVS, Galetin A and Houston JB (2018) Predicting Human

Clearance of Organic Anion Transporting Polypeptide Substrates Using Cynomolgus Monkey: In Vitro-In Vivo Scaling of Hepatic Uptake Clearance. *Drug Metab Dispos* 46: 989-1000.

Deng R, Iyer S, Theil FP, Mortensen DL, Fielder PJ and Prabhu S (2011) Projecting human pharmacokinetics of therapeutic antibodies from nonclinical data: what have we learned? *MAbs* 3: 61-66.

Drozdzik M, Groer C, Penski J, Lapczuk J, Ostrowski M, Lai Y, Prasad B, Unadkat JD, Siegmund W and Oswald S (2014) Protein abundance of clinically relevant multidrug transporters along the entire length of the human intestine. *Mol Pharm* 11: 3547-3555.

Duan P, Zhao P and Zhang L (2017) Physiologically Based Pharmacokinetic (PBPK) Modeling of Pitavastatin and Atorvastatin to Predict Drug-Drug Interactions (DDIs). *Eur J Drug Metab Pharmacokinet* 42: 689-705.

Ebeling M, Kung E, See A, Broger C, Steiner G, Berrera M, Heckel T, Iniguez L, Albert T, Schmucki R, Biller H, Singer T and Certa U (2011) Genome-based analysis of the nonhuman primate Macaca fascicularis as a model for drug safety assessment. *Genome Res* 21: 1746-1756.

Emoto C, Yoda N, Uno Y, Iwasaki K, Umehara K, Kashiyama E and Yamazaki H (2013) Comparison of p450 enzymes between cynomolgus monkeys and humans: p450 identities, protein contents, kinetic parameters, and potential for inhibitory profiles. *Curr Drug Metab* 14: 239-252.

Eng H, Bi YA, West MA, Ryu S, Yamaguchi E, Kosa RE, Tess DA, Griffith DA, Litchfield J, Kalgutkar AS and Varma MVS (2021) Organic Anion-Transporting Polypeptide 1B1/1B3-Mediated Hepatic Uptake Determines the Pharmacokinetics of Large

Lipophilic Acids: In Vitro-In Vivo Evaluation in Cynomolgus Monkey. *J Pharmacol Exp Ther* 377: 169-180.

Ferguson B, Street SL, Wright H, Pearson C, Jia Y, Thompson SL, Allibone P, Dubay CJ, Spindel E and Norgren RB, Jr. (2007) Single nucleotide polymorphisms (SNPs) distinguish Indian-origin and Chinese-origin rhesus macaques (Macaca mulatta). *BMC Genomics* 8: 43.

Gisclon LG, Boyd RA, Williams RL and Giacomini KM (1989) The effect of probenecid on the renal elimination of cimetidine. *Clin Pharmacol Ther* 45: 444-452.

Gu X, Wang L, Gan J, Fancher RM, Tian Y, Hong Y, Lai Y, Sinz M and Shen H (2020) Absorption and Disposition of Coproporphyrin I (CPI) in Cynomolgus Monkeys and Mice: Pharmacokinetic Evidence to Support the Use of CPI to Inform the Potential for Organic Anion-Transporting Polypeptide Inhibition. *Drug Metab Dispos* 48: 724-734.

Gui C and Hagenbuch B (2010) Cloning/characterization of the canine organic anion transporting polypeptide 1b4 (Oatp1b4) and classification of the canine OATP/SLCO members. *Comp Biochem Physiol C Toxicol Pharmacol* 151: 393-399.

Hagenbuch B and Gui C (2008) Xenobiotic transporters of the human organic anion transporting polypeptides (OATP) family. *Xenobiotica* 38: 778-801.

Hammer H, Schmidt F, Marx-Stoelting P, Potz O and Braeuning A (2021) Cross-species analysis of hepatic cytochrome P450 and transport protein expression. *Arch Toxicol* 95: 117-133.

Harwood MD, Achour B, Russell MR, Carlson GL, Warhurst G and Rostami-Hodjegan A (2015) Application of an LC-MS/MS method for the simultaneous quantification of

human intestinal transporter proteins absolute abundance using a QconCAT technique. *J Pharm Biomed Anal* 110: 27-33.

Harwood MD, Zhang M, Pathak SM and Neuhoff S (2019) The Regional-Specific Relative and Absolute Expression of Gut Transporters in Adult Caucasians: A Meta-Analysis. *Drug Metab Dispos* 47: 854-864.

He YJ, Zhang W, Chen Y, Guo D, Tu JH, Xu LY, Tan ZR, Chen BL, Li Z, Zhou G, Yu BN, Kirchheiner J and Zhou HH (2009) Rifampicin alters atorvastatin plasma concentration on the basis of SLCO1B1 521T>C polymorphism. *Clin Chim Acta* 405: 49-52.

Hediger MA, Clemencon B, Burrier RE and Bruford EA (2013) The ABCs of membrane transporters in health and disease (SLC series): introduction. *Mol Aspects Med* 34: 95-107.

Inotsume N, Nishimura M, Nakano M, Fujiyama S and Sato T (1990) The inhibitory effect of probenecid on renal excretion of famotidine in young, healthy volunteers. *J Clin Pharmacol* 30: 50-56.

International Transporter C, Giacomini KM, Huang SM, Tweedie DJ, Benet LZ, Brouwer KL, Chu X, Dahlin A, Evers R, Fischer V, Hillgren KM, Hoffmaster KA, Ishikawa T, Keppler D, Kim RB, Lee CA, Niemi M, Polli JW, Sugiyama Y, Swaan PW, Ware JA, Wright SH, Yee SW, Zamek-Gliszczynski MJ and Zhang L (2010) Membrane transporters in drug development. *Nat Rev Drug Discov* 9: 215-236.

Ito K, Uchida Y, Ohtsuki S, Aizawa S, Kawakami H, Katsukura Y, Kamiie J and Terasaki T (2011) Quantitative membrane protein expression at the blood-brain barrier of adult and younger cynomolgus monkeys. *J Pharm Sci* 100: 3939-3950.

Jones HM, Barton HA, Lai Y, Bi YA, Kimoto E, Kempshall S, Tate SC, El-Kattan A, Houston JB, Galetin A and Fenner KS (2012) Mechanistic pharmacokinetic modeling for the prediction of transporter-mediated disposition in humans from sandwich culture human hepatocyte data. *Drug Metab Dispos* 40: 1007-1017.

Kanehisa M, Goto S, Furumichi M, Tanabe M and Hirakawa M (2010) KEGG for representation and analysis of molecular networks involving diseases and drugs. *Nucleic Acids Res* 38: D355-360.

Karibe T, Hagihara-Nakagomi R, Abe K, Imaoka T, Mikkaichi T, Yasuda S, Hirouchi M, Watanabe N, Okudaira N and Izumi T (2015) Evaluation of the usefulness of breast cancer resistance protein (BCRP) knockout mice and BCRP inhibitor-treated monkeys to estimate the clinical impact of BCRP modulation on the pharmacokinetics of BCRP substrates. *Pharm Res* 32: 1634-1647.

Karibe T, Imaoka T, Abe K and Ando O (2018) Curcumin as an In Vivo Selective Intestinal Breast Cancer Resistance Protein Inhibitor in Cynomolgus Monkeys. *Drug Metab Dispos* 46: 667-679.

Kim S, Dinchuk JE, Anthony MN, Orcutt T, Zoeckler ME, Sauer MB, Mosure KW, Vuppugalla R, Grace JE, Jr., Simmermacher J, Dulac HA, Pizzano J and Sinz M (2010) Evaluation of cynomolgus monkey pregnane X receptor, primary hepatocyte, and in vivo pharmacokinetic changes in predicting human CYP3A4 induction. *Drug Metab Dispos* 38: 16-24.

Kimoto E, Bi YA, Kosa RE, Tremaine LM and Varma MVS (2017) Hepatobiliary Clearance Prediction: Species Scaling From Monkey, Dog, and Rat, and In Vitro-In Vivo

Extrapolation of Sandwich-Cultured Human Hepatocytes Using 17 Drugs. *J Pharm Sci* 106: 2795-2804.

Kosa RE, Lazzaro S, Bi YA, Tierney B, Gates D, Modi S, Costales C, Rodrigues AD, Tremaine LM and Varma MV (2018) Simultaneous Assessment of Transporter-Mediated Drug-Drug Interactions Using a Probe Drug Cocktail in Cynomolgus Monkey. *Drug Metab Dispos* 46: 1179-1189.

Kusuhara H, Furuie H, Inano A, Sunagawa A, Yamada S, Wu C, Fukizawa S, Morimoto N, Ieiri I, Morishita M, Sumita K, Mayahara H, Fujita T, Maeda K and Sugiyama Y (2012) Pharmacokinetic interaction study of sulphasalazine in healthy subjects and the impact of curcumin as an in vivo inhibitor of BCRP. *Br J Pharmacol* 166: 1793-1803.

Lai Y, Mandlekar S, Shen H, Holenarsipur VK, Langish R, Rajanna P, Murugesan S, Gaud N, Selvam S, Date O, Cheng Y, Shipkova P, Dai J, Humphreys WG and Marathe P (2016) Coproporphyrins in Plasma and Urine Can Be Appropriate Clinical Biomarkers to Recapitulate Drug-Drug Interactions Mediated by Organic Anion Transporting Polypeptide Inhibition. *J Pharmacol Exp Ther* 358: 397-404.

Lau YY, Huang Y, Frassetto L and Benet LZ (2007) effect of OATP1B transporter inhibition on the pharmacokinetics of atorvastatin in healthy volunteers. *Clin Pharmacol Ther* 81: 194-204.

Lee SC, Arya V, Yang X, Volpe DA and Zhang L (2017) Evaluation of transporters in drug development: Current status and contemporary issues. *Adv Drug Deliv Rev* 116: 100-118.

Li N, Palandra J, Nemirovskiy OV and Lai Y (2009a) LC-MS/MS mediated absolute quantification and comparison of bile salt export pump and breast cancer resistance protein in livers and hepatocytes across species. *Anal Chem* 81: 2251-2259.

Li N, Zhang Y, Hua F and Lai Y (2009b) Absolute difference of hepatobiliary transporter multidrug resistance-associated protein (MRP2/Mrp2) in liver tissues and isolated hepatocytes from rat, dog, monkey, and human. *Drug Metab Dispos* 37: 66-73.

Liang X and Lai Y (2021) Overcoming the shortcomings of the extended-clearance concept: a framework for developing a physiologically-based pharmacokinetic (PBPK) model to select drug candidates involving transporter-mediated clearance. *Expert Opin Drug Metab Toxicol* 17: 869-886.

Liang X, Park Y, DeForest N, Hao J, Zhao X, Niu C, Wang K, Smith B and Lai Y (2020) In Vitro Hepatic Uptake in Human and Monkey Hepatocytes in the Presence and Absence of Serum Protein and Its In Vitro to In Vivo Extrapolation. *Drug Metab Dispos* 48: 1283-1292.

Matsunaga N, Ufuk A, Morse BL, Bedwell DW, Bao J, Mohutsky MA, Hillgren KM, Hall SD, Houston JB and Galetin A (2019) Hepatic Organic Anion Transporting Polypeptide-Mediated Clearance in the Beagle Dog: Assessing In Vitro-In Vivo Relationships and Applying Cross-Species Empirical Scaling Factors to Improve Prediction of Human Clearance. *Drug Metab Dispos* 47: 215-226.

Mizuno N, Niwa T, Yotsumoto Y and Sugiyama Y (2003) Impact of drug transporter studies on drug discovery and development. *Pharmacol Rev* 55: 425-461.

Mochizuki T, Mizuno T, Maeda K and Kusuhara H (2021) Current progress in identifying endogenous biomarker candidates for drug transporter phenotyping and their potential application to drug development. *Drug Metab Pharmacokinet* 37: 100358.

Mori D, Kimoto E, Rago B, Kondo Y, King-Ahmad A, Ramanathan R, Wood LS, Johnson JG, Le VH, Vourvahis M, David Rodrigues A, Muto C, Furihata K, Sugiyama Y and Kusuhara H (2020) Dose-Dependent Inhibition of OATP1B by Rifampicin in Healthy Volunteers: Comprehensive Evaluation of Candidate Biomarkers and OATP1B Probe Drugs. *Clin Pharmacol Ther* 107: 1004-1013.

Morse BL, Cai H, MacGuire JG, Fox M, Zhang L, Zhang Y, Gu X, Shen H, Dierks EA, Su H, Luk CE, Marathe P, Shu YZ, Humphreys WG and Lai Y (2015) Rosuvastatin Liver Partitioning in Cynomolgus Monkeys: Measurement In Vivo and Prediction Using In Vitro Monkey Hepatocyte Uptake. *Drug Metab Dispos* 43: 1788-1794.

Morse BL, Fallon JK, Kolur A, Hogan AT, Smith PC and Hillgren KM (2021) Comparison of Hepatic Transporter Tissue Expression in Rodents and Interspecies Hepatic OCT1 Activity. *AAPS J* 23: 58.

Morse BL, MacGuire JG, Marino AM, Zhao Y, Fox M, Zhang Y, Shen H, Griffith Humphreys W, Marathe P and Lai Y (2017) Physiologically Based Pharmacokinetic Modeling of Transporter-Mediated Hepatic Clearance and Liver Partitioning of OATP and OCT Substrates in Cynomolgus Monkeys. *AAPS J* 19: 1878-1889.

Nakamura K, Hirayama-Kurogi M, Ito S, Kuno T, Yoneyama T, Obuchi W, Terasaki T and Ohtsuki S (2016) Large-scale multiplex absolute protein quantification of drug-metabolizing enzymes and transporters in human intestine, liver, and kidney

microsomes by SWATH-MS: Comparison with MRM/SRM and HR-MRM/PRM. *Proteomics* 16: 2106-2117.

Niu C, Wang Y, Zhao X, Tep S, Murakami E, Subramanian R, Smith B and Lai Y (2019) Organic Anion-Transporting Polypeptide Genes Are Not Induced by the Pregnane X Receptor Activator Rifampin: Studies in Hepatocytes In Vitro and in Monkeys In Vivo. *Drug Metab Dispos* 47: 1433-1442.

Nozaki Y and Izumi S (2020) Recent advances in preclinical in vitro approaches towards quantitative prediction of hepatic clearance and drug-drug interactions involving organic anion transporting polypeptide (OATP) 1B transporters. *Drug Metab Pharmacokinet* 35: 56-70.

Ogawa SI, Shimizu M, Kamiya Y, Uehara S, Suemizu H and Yamazaki H (2020a) Increased plasma concentrations of an antidyslipidemic drug pemafibrate co-administered with rifampicin or cyclosporine A in cynomolgus monkeys genotyped for the organic anion transporting polypeptide 1B1. *Drug Metab Pharmacokinet* 35: 354-360.

Ogawa SI, Shimizu M and Yamazaki H (2020b) Plasma concentrations of pemafibrate with co-administered drugs predicted by physiologically based pharmacokinetic modeling in virtual populations with renal/hepatic impairment. *Xenobiotica* 50: 1023-1031.

Ogawa SI, Tsunenari Y, Kawai H and Yamazaki H (2019) Pharmacokinetics and metabolism of pemafibrate, a novel selective peroxisome proliferator-activated receptor-alpha modulator, in rats and monkeys. *Biopharm Drug Dispos* 40: 12-17.

Ohtsuki S, Schaefer O, Kawakami H, Inoue T, Liehner S, Saito A, Ishiguro N, Kishimoto W, Ludwig-Schwellinger E, Ebner T and Terasaki T (2012) Simultaneous absolute protein quantification of transporters, cytochromes P450, and UDP-glucuronosyltransferases as

a novel approach for the characterization of individual human liver: comparison with mRNA levels and activities. *Drug Metab Dispos* 40: 83-92.

Perelman P, Johnson WE, Roos C, Seuanez HN, Horvath JE, Moreira MA, Kessing B, Pontius J, Roelke M, Rumpler Y, Schneider MP, Silva A, O'Brien SJ and Pecon-Slattery J (2011) A molecular phylogeny of living primates. *PLoS Genet* 7: e1001342.

Peters SA, Jones CR, Ungell AL and Hatley OJ (2016) Predicting Drug Extraction in the Human Gut Wall: Assessing Contributions from Drug Metabolizing Enzymes and Transporter Proteins using Preclinical Models. *Clin Pharmacokinet* 55: 673-696.

Prasad B, Lai Y, Lin Y and Unadkat JD (2013) Interindividual variability in the hepatic expression of the human breast cancer resistance protein (BCRP/ABCG2): effect of age, sex, and genotype. *J Pharm Sci* 102: 787-793.

Qiu X, Bi YA, Balogh LM and Lai Y (2013) Absolute measurement of species differences in sodium taurocholate cotransporting polypeptide (NTCP/Ntcp) and its modulation in cultured hepatocytes. *J Pharm Sci* 102: 3252-3263.

Rodrigues AD, Taskar KS, Kusuhara H and Sugiyama Y (2018) Endogenous Probes for Drug Transporters: Balancing Vision With Reality. *Clin Pharmacol Ther* 103: 434-448.

Shen H, Christopher L, Lai Y, Gong J, Kandoussi H, Garonzik S, Perera V, Garimella T and Humphreys WG (2018a) Further Studies to Support the Use of Coproporphyrin I and III as Novel Clinical Biomarkers for Evaluating the Potential for Organic Anion Transporting Polypeptide (OATP) 1B1 and OATP1B3 Inhibition. *Drug Metab Dispos*.

Shen H, Dai J, Liu T, Cheng Y, Chen W, Freeden C, Zhang Y, Humphreys WG, Marathe P and Lai Y (2016a) Coproporphyrins I and III as Functional Markers of OATP1B

Activity: In Vitro and In Vivo Evaluation in Preclinical Species. *J Pharmacol Exp Ther* 357: 382-393.

Shen H, Holenarsipur VK, Mariappan TT, Drexler DM, Cantone JL, Rajanna P, Singh Gautam S, Zhang Y, Gan J, Shipkova PA, Marathe P and Humphreys WG (2019a) Evidence for the Validity of Pyridoxic Acid (PDA) as a Plasma-Based Endogenous Probe for OAT1 and OAT3 Function in Healthy Subjects. *J Pharmacol Exp Ther* 368: 136-145.

Shen H, Liu T, Jiang H, Titsch C, Taylor K, Kandoussi H, Qiu X, Chen C, Sukrutharaj S, Kuit K, Mintier G, Krishnamurthy P, Fancher RM, Zeng J, Rodrigues AD, Marathe P and Lai Y (2016b) Cynomolgus Monkey as a Clinically Relevant Model to Study Transport Involving Renal Organic Cation Transporters: In Vitro and In Vivo Evaluation. *Drug Metab Dispos* 44: 238-249.

Shen H, Nelson DM, Oliveira RV, Zhang Y, McNaney CA, Gu X, Chen W, Su C, Reily MD, Shipkova PA, Gan J, Lai Y, Marathe P and Humphreys WG (2018b) Discovery and Validation of Pyridoxic Acid and Homovanillic Acid as Novel Endogenous Plasma Biomarkers of Organic Anion Transporter (OAT) 1 and OAT3 in Cynomolgus Monkeys. *Drug Metab Dispos* 46: 178-188.

Shen H, Scialis RJ and Lehman-McKeeman L (2019b) Xenobiotic Transporters in the Kidney: Function and Role in Toxicity. *Semin Nephrol* 39: 159-175.

Shen H, Su H, Liu T, Yao M, Mintier G, Li L, Fancher RM, Iyer R, Marathe P, Lai Y and Rodrigues AD (2015) Evaluation of rosuvastatin as an organic anion transporting polypeptide (OATP) probe substrate: in vitro transport and in vivo disposition in cynomolgus monkeys. *J Pharmacol Exp Ther* 353: 380-391.

Shen H, Yang Z, Mintier G, Han YH, Chen C, Balimane P, Jemal M, Zhao W, Zhang R, Kallipatti S, Selvam S, Sukrutharaj S, Krishnamurthy P, Marathe P and Rodrigues AD (2013) Cynomolgus monkey as a potential model to assess drug interactions involving hepatic organic anion transporting polypeptides: in vitro, in vivo, and in vitro-to-in vivo extrapolation. *J Pharmacol Exp Ther* 344: 673-685.

Sheps JA and Ling V (2007) Preface: the concept and consequences of multidrug resistance. *Pflugers Arch* 453: 545-553.

Shida S, Utoh M, Murayama N, Shimizu M, Uno Y and Yamazaki H (2015) Human plasma concentrations of cytochrome P450 probes extrapolated from pharmacokinetics in cynomolgus monkeys using physiologically based pharmacokinetic modeling. *Xenobiotica* 45: 881-886.

Smith DE, Gee WL, Brater DC, Lin ET and Benet LZ (1980) Preliminary evaluation of furosemide-probenecid interaction in humans. *J Pharm Sci* 69: 571-575.

Stokes WS (2015) Animals and the 3Rs in toxicology research and testing: The way forward. *Hum Exp Toxicol* 34: 1297-1303.

Storelli F, Billington S, Kumar AR and Unadkat JD (2021) Abundance of P-Glycoprotein and Other Drug Transporters at the Human Blood-Brain Barrier in Alzheimer's Disease: A Quantitative Targeted Proteomic Study. *Clin Pharmacol Ther* 109: 667-675.

Syvanen S, Lindhe O, Palner M, Kornum BR, Rahman O, Langstrom B, Knudsen GM and Hammarlund-Udenaes M (2009) Species differences in blood-brain barrier transport of three positron emission tomography radioligands with emphasis on P-glycoprotein transport. *Drug Metab Dispos* 37: 635-643.

Tahara H, Kusuhara H, Chida M, Fuse E and Sugiyama Y (2006) Is the monkey an appropriate animal model to examine drug-drug interactions involving renal clearance? Effect of probenecid on the renal elimination of H2 receptor antagonists. *J Pharmacol Exp Ther* 316: 1187-1194.

Tahara H, Shono M, Kusuhara H, Kinoshita H, Fuse E, Takadate A, Otagiri M and Sugiyama Y (2005) Molecular cloning and functional analyses of OAT1 and OAT3 from cynomolgus monkey kidney. *Pharm Res* 22: 647-660.

Takahashi M, Washio T, Suzuki N, Igeta K, Fujii Y, Hayashi M, Shirasaka Y and Yamashita S (2008) Characterization of gastrointestinal drug absorption in cynomolgus monkeys. *Mol Pharm* 5: 340-348.

Takahashi T, Ohtsuka T, Uno Y, Utoh M, Yamazaki H and Kume T (2016) Pre-incubation with cyclosporine A potentiates its inhibitory effects on pitavastatin uptake mediated by recombinantly expressed cynomolgus monkey hepatic organic anion transporting polypeptide. *Biopharm Drug Dispos* 37: 479-490.

Takahashi T, Ohtsuka T, Yoshikawa T, Tatekawa I, Uno Y, Utoh M, Yamazaki H and Kume T (2013) Pitavastatin as an in vivo probe for studying hepatic organic anion transporting polypeptide-mediated drug-drug interactions in cynomolgus monkeys. *Drug Metab Dispos* 41: 1875-1882.

Takahashi T, Uno Y, Yamazaki H and Kume T (2019) Functional characterization for polymorphic organic anion transporting polypeptides (OATP/SLCO1B1, 1B3, 2B1) of monkeys recombinantly expressed with various OATP probes. *Biopharm Drug Dispos* 40: 62-69.

Takehara I, Watanabe N, Mori D, Ando O and Kusuhara H (2019) Effect of Rifampicin on the Plasma Concentrations of Bile Acid-O-Sulfates in Monkeys and Human Liver-Transplanted Chimeric Mice With or Without Bile Flow Diversion. *J Pharm Sci* 108: 2756-2764.

Takehara I, Yoshikado T, Ishigame K, Mori D, Furihata KI, Watanabe N, Ando O, Maeda K, Sugiyama Y and Kusuhara H (2018) Comparative Study of the Dose-Dependence of OATP1B Inhibition by Rifampicin Using Probe Drugs and Endogenous Substrates in Healthy Volunteers. *Pharm Res* 35: 138.

Tang C and Prueksaritanont T (2010) Use of in vivo animal models to assess pharmacokinetic drug-drug interactions. *Pharm Res* 27: 1772-1787.

Taskar KS, Pilla Reddy V, Burt H, Posada MM, Varma M, Zheng M, Ullah M, Emami Riedmaier A, Umehara KI, Snoeys J, Nakakariya M, Chu X, Beneton M, Chen Y, Huth F, Narayanan R, Mukherjee D, Dixit V, Sugiyama Y and Neuhoff S (2020) Physiologically-Based Pharmacokinetic Models for Evaluating Membrane Transporter Mediated Drug-Drug Interactions: Current Capabilities, Case Studies, Future Opportunities, and Recommendations. *Clin Pharmacol Ther* 107: 1082-1115.

Thakare R, Gao H, Kosa RE, Bi YA, Varma MV, Cerny M, Sharma R, Kuhn M, Huang B, Liu Y, Yu A, Walker GS, Niosi M, Tremaine LM, Alnouti Y and Rodrigues AD (2017) Leveraging of Rifampicin-Dosed Cynomolgus Monkeys to Identify Bile Acid 3-O-Sulfate Conjugates as Potential Novel Biomarkers for Organic Anion-Transporting Polypeptides. *Drug Metab Dispos*.

Uchida Y, Ohtsuki S, Katsukura Y, Ikeda C, Suzuki T, Kamiie J and Terasaki T (2011) Quantitative targeted absolute proteomics of human blood-brain barrier transporters and receptors. *J Neurochem* 117: 333-345.

Uchida Y, Wakayama K, Ohtsuki S, Chiba M, Ohe T, Ishii Y and Terasaki T (2014) Blood-brain barrier pharmacoproteomics-based reconstruction of the in vivo brain distribution of P-glycoprotein substrates in cynomolgus monkeys. *J Pharmacol Exp Ther* 350: 578-588.

Ufuk A, Kosa RE, Gao H, Bi YA, Modi S, Gates D, Rodrigues AD, Tremaine LM, Varma MVS, Houston JB and Galetin A (2018) In Vitro-In Vivo Extrapolation of OATP1B-Mediated Drug-Drug Interactions in Cynomolgus Monkey. *J Pharmacol Exp Ther* 365: 688-699.

Uno Y, Fujino H, Kito G, Kamataki T and Nagata R (2006) CYP2C76, a novel cytochrome P450 in cynomolgus monkey, is a major CYP2C in liver, metabolizing tolbutamide and testosterone. *Mol Pharmacol* 70: 477-486.

Uno Y, Iwasaki K, Yamazaki H and Nelson DR (2011) Macaque cytochromes P450: nomenclature, transcript, gene, genomic structure, and function. *Drug Metab Rev* 43: 346-361.

Wang L, Prasad B, Salphati L, Chu X, Gupta A, Hop CE, Evers R and Unadkat JD (2015) Interspecies variability in expression of hepatobiliary transporters across human, dog, monkey, and rat as determined by quantitative proteomics. *Drug Metab Dispos* 43: 367-374.

Weidekamm E, Plozza-Nottebrock H, Forgo I and Dubach UC (1982) Plasma concentrations in pyrimethamine and sulfadoxine and evaluation of pharmacokinetic data by computerized curve fitting. *Bull World Health Organ* 60: 115-122.

Wiebe ST, Giessmann T, Hohl K, Schmidt-Gerets S, Hauel E, Jambrecina A, Bader K, Ishiguro N, Taub ME, Sharma A, Ebner T, Mikus G, Fromm MF, Muller F and Stopfer P (2020) Validation of a Drug Transporter Probe Cocktail Using the Prototypical Inhibitors Rifampin, Probenecid, Verapamil, and Cimetidine. *Clin Pharmacokinet* 59: 1627-1639.

Yasunaga M, Takemura M, Fujita K, Yabuuchi H and Wada M (2008) Molecular cloning and functional characterization of cynomolgus monkey multidrug resistance-associated protein 2 (MRP2). *Eur J Pharm Sci* 35: 326-334.

Ye AY, Liu QR, Li CY, Zhao M and Qu H (2014) Human transporter database: comprehensive knowledge and discovery tools in the human transporter genes. *PLoS One* 9: e88883.

Zamek-Gliszczynski MJ, Bedwell DW, Bao JQ and Higgins JW (2012) Characterization of SAGE Mdr1a (P-gp), Bcrp, and Mrp2 knockout rats using loperamide, paclitaxel, sulfasalazine, and carboxydichlorofluorescein pharmacokinetics. *Drug Metab Dispos* 40: 1825-1833.

Zhang Y, Chen C, Chen SJ, Chen XQ, Shuster DJ, Puszczalo PD, Fancher RM, Yang Z, Sinz M and Shen H (2020a) Absence of OATP1B (Organic Anion-Transporting Polypeptide) Induction by Rifampin in Cynomolgus Monkeys: Determination Using the Endogenous OATP1B Marker Coproporphyrin and Tissue Gene Expression. *J Pharmacol Exp Ther* 375: 139-151.

Zhang Y, Holenarsipur VK, Kandoussi H, Zeng J, Mariappan TT, Sinz M and Shen H (2020b) Detection of Weak Organic Anion-Transporting Polypeptide 1B Inhibition by Probenecid with Plasma-Based Coproporphyrin in Humans. *Drug Metab Dispos* 48: 841-848.

Zhang Y, Panfen E, Fancher M, Sinz M, Marathe P and Shen H (2019) Dissecting the Contribution of OATP1B1 to Hepatic Uptake of Statins Using the OATP1B1 Selective Inhibitor Estropipate. *Mol Pharm* 16: 2342-2353.

Footnotes

Reprint requests:

- **Dr. Hong Shen,** Associate Director

  Department of Metabolism and Pharmacokinetics, Bristol Myers Squibb Company

  Route 206 & Province Line Road, Princeton, NJ 08543

  Telephone: (609) 252-4509

  E-mail: hong.shen1@bms.com

- This study is supported by Bristol Myers Squibb Company.

DMD Fast Forward. Published on December 10, 2021 as DOI: 10.1124/dmd.121.000695
This article has not been copyedited and formatted. The final version may differ from this version.

Figure Legends

Figure 1. Schematic diagram of translational research using cynomolgus monkey transporter models. Different monkey models are used as nonclinical models of transporter-mediated drug disposition and interaction investigations. Abbreviation: CPI, coproporphyrin I; DDI, drug-drug interaction; PDA, pyridoxic acid.

Figure 2. Summary of available published cross-species uptake and efflux transporter expression data in the liver (A and B, respectively) and kidneys (C and D, respectively). Mean expression data of transporters in the tissues of humans (blue box), cynomolgus monkeys (red box), Sprague-Dawley rats (green box), beagle dogs (brown box) and mice (yellow box) were obtained from Wang et al. (2015) and Basit et al. (2019). Boxes represent the ranges of transporter protein expressions.

Figure 3. Comparison of available published K_m (A and B) and IC_{50} values (C and D) of reference substrates and inhibitors between cynomolgus monkey and human transporters. Summary of the data presented in Table 3 (K_m values of 20 substrates) and Table 4 (K_i and IC_{50} values of 72 inhibitors). The solid and dotted lines represent the line of unity and the 33 to 300% range of the observed value, respectively.

Figure 4. Comparison of available published pharmacokinetic DDI mediated by OATP1B (A), BCRP (B), OAT1/3 (C), and OCT2-MATE inhibition (D) as well as renal clearance between cynomolgus monkey and human transporters. Summary of the area under the plasma concentration-time curve ratios (AUCR) and renal clearance (CL_R) ratios of victim drug

substrates presented in Table 5. Open blue circle and red square data points represent the AUCR and CL_R ratio of individual cynomolgus monkey and human study, respectively. Box and error bar depict mean and standard deviation (SD), respectively.

Table 1. The major advantages, disadvantages, and challenges of using cynomolgus monkey transporter models in support of drug transporter research.

Property		Advantages and Limitations of Monkey Transporter Models
Advantages	*Genetics*	Share ideal identity with greater than 90 percent of the DNA sequences of human drug transport systems that other mammalian species may lack [e.g., SLCO1B1 (OATP1B1 gene) and SLC47A2 (MATE2-K gene)]
	Transport characteristics	Monkey is most similar to human with respect to substrate specificity, transport kinetics, and transporter inhibition potency
	Pharmacokinetic investigation	Display similar physiology and biochemistry properties compared with humans and have larger body size than rodent experimental models, making them suitable for pharmacokinetics disposition and drug interaction investigations
	Transporter regulation	Share greater similarities with humans in nuclear receptor functional regulation associated with transporters and drug-metabolizing enzymes (e.g., rifampin induction)
	Translational sciences	Recapture numerous clinical transporter DDIs, and enable translation of vitro and animal data to clinical findings and confirming transport mechanism
Disadvantages/Challenges	*Transporter expression and activities*	There are likely species-dependent difference in transporter expression, transport kinetics, and substrate specificity between cynomolgus monkey and human
	In vitro monkey transporter reagents	In vitro transfected cell and membrane vesicle models are not widely available
	Genetic background and variation	There are likely differences in some transporter gene sequences that have been encountered within cynomolgus monkeys sourced from different geographic origins (e.g., China, the Philippines, and Mauritius)

Table 2. Amino acid sequence identity between human, cynomolgus monkey, mouse, rat and dog transporters.

Gene Family	Human Protein (Gene Symbol)	GenBank Accession Number	Amino Acid Sequence Identity (GenBank Accession Number)				Cynomolgus Monkey Transporter References
			Cynomolgus Monkey	Mouse	Rat	Dog	
SLCO	OATP1B1 (*SLCO1B1*)	NM_006446	92% (Oatp1b1) (JX866725)	65% (Oatp1b2) (NM_020495)	64% (Oatp1b2) (NM_031650)	69% (Oatp1b4) (GQ497899)	Shen et al., 2013, Takahashi et al., 2019
	OATP1B3 (*SLCO1B3*)	NM_019844	94% (Oatp1b3) (JX866726)	No homologue	No homologue	No homologue	Shen et al., 2013
	OATP2B1 (*SLCO2B1*)	NM_007256	97% (JX866727)	76% (NM_001252530)	76% (NM_080786)	80% (XM_005633497)	Shen et al., 2013
ABCB	MDR1 (P-gp) (*ABCB1*)	NM_000927	96% (Mdr1) (NM_001287322)	87% (Mdr1a) (NM_011076) 84% (Mdr1b) (NM_011075)	74% (Mdr1a) (XM_006235994) 66% (Mdr1b) (XM_017592469)	75% (Mdr1) (NM_001003215)	Kosa, 2018
ABCC	MRP2 (*ABCC2*)	NM_000392	96% (NM_001287716)	78% (NM_013806)	78% (NM_012833)	83% (NM_001003081)	Yasunaga et al., 2008
ABCG	BCRP (*ABCG2*)	NM_001257386	97% (XM_005555388)	81% (NM_001355477)	81% (XM_006236576)	83% (NM_001048021)	Kosa, 2018
SLC22A	OCT1 (*SLC22A1*)	NM_003057	92% (BMS data)	78% (NM_009202)	51% (NM_012697)	74% (XM_022425124)	In-house data
	OCT2 (*SLC22A2*)	NM_003058	94% (KP731382)	71% (NM_001355767)	69% (NM_031584)	69% (NM_001286961)	Shen et al., 2016
	OAT1 (*SLC22A6*)	XM_017018562	97% (NM_001287697)	76% (NM_008766)	80% (XM_006230978)	91% (XM_533258)	Tahara et al., 2005
	OAT2 (*SLC22A7*)	NM_006672	97% (BMS data)	79% (NM_144856)	79% (NM_053537)	72% (XM_022426070)	In-house data
	OAT3 (*SLC22A8*)	NM_001184732	95% (AB182993)	77% (NM_001164634)	79% (NM_031332)	78% (XM_005631595)	Tahara et al., 2005
SLC47A	MATE1 (*SLC47A1*)	NM_018242	95% (KP731383)	78% (NM_026183)	78% (NM_001014118)	? (XM_022418634)	Shen et al., 2016
	MATE2-K (*SLC22A2*)	NM_001099646	96% (KP731384)	No homologue	No homologue	70% (XM_014113641)	Shen et al., 2016

Note: The percentages of identity among the various amino acid sequences were determined using BLAST alignment analysis (https://blast.ncbi.nlm.nih.gov/Blast.cgi); BCRP, breast cancer resistance protein; MATE, multidrug and toxin extrusion; MDR, multidrug resistance protein; OAT, organic anion transporter; OATP, organic anion transporting polypeptide; OCT, organic cation transporter.

Table 3. Summary of literature reports describing Michaelis-Menten constant (K_m) values for different substrates with cynomolgus monkey and human transporters.

Transporter	Substrate	In Vitro System	Transport K_m (μM)		Ratio	References
			Cynomolgus Monkey	Human		
OATP1B1	Rosuvastatin	HEK-293	14.4	15.3	1.1	Shen et al., 2013
OATP1B3	Rosuvastatin	HEK-293	14.5	13.5	0.9	Shen et al., 2013
OATP2B1	Rosuvastatin	HEK-293	9.6	10.6	1.1	Shen et al., 2013
OATPs & NTCP	Rosuvastatin	Hepatocytes	6.7	10.3	1.5	Shen et al., 2013
OAT1	*p*-Aminohippurate	HEK-293	10.1	20.4	2.0	Tahara et al., 2005
	2,4-Dichloro-phenoxyacetate	HEK-293	3.00	5.77	1.9	Tahara et al., 2005
	Hippurate	HEK-293	12.2	23.5	1.9	Tahara et al., 2005
	Indoleacetate	HEK-293	23.6	14.0	0.6	Tahara et al., 2005
	Indoxyl sulfate	HEK-293	32.9	20.5	0.6	Tahara et al., 2005
	CMPF	HEK-293	85.3	141	1.7	Tahara et al., 2005
OAT3	Benzylpenicillin	HEK-293	49.2	52.1	1	Tahara et al., 2005
	Estrone 3 sulfate	HEK-293	10.6	9.51	0.9	Tahara et al., 2005
	CMPF	HEK-293	18.6	26.5	1.4	Tahara et al., 2005
	Cimetidine	HEK-293	68.5	113	1.6	Tahara et al., 2005
	Cimetidine	HEK-293	70.9	149	2.1	Tahara et al., 2006
	Famotidine	HEK-293	154	124	0.8	Tahara et al., 2006
	Ranitidine	HEK-293	125	234	1.9	Tahara et al., 2006
OCT2	Metformin	HEK-293	628	1465	2.3	Shen et al., 2016
MATE1	Metformin	HEK-293	340	228	0.7	Shen et al., 2016
MATE2-K	Metformin	HEK-293	1566	819	0.5	Shen et al., 2016

Note: HEK-293, human embryonic kidney 293 cells; K_m, Michaelis-Menten constant that corresponds to the substrate concentration at which the

uptake rate is half of maximal transport rate; MATE, multidrug and toxin extrusion; NTCP, sodium-taurocholate co-transporting polypeptide; OAT, organic anion transporter; OATP, organic anion transporting polypeptide; OCT, organic cation transporter.

Table 4. Summary of literature reports describing IC_{50} values for various inhibitors of cynomolgus monkey and human transporters.

Transporter	Inhibitor	In Vitro System	Probe	IC_{50} (μM)		*Ratio*	References
				Cynomolgus Monkey	Human		
OATP1B1	Rifampin	HEK-293	E17βG	0.20	0.55	2.8	Shen et al., 2013
		HEK-293	Rosuvastatin	0.42	1.10	2.6	Shen et al., 2013
		HEK-293	E17βG	0.38	0.60	1.6	Chu et al., 2015
		HEK-293	Rosuvastatin	0.59	0.63	1.1	Zhang et al., 2019
	Rifamycin SV	HEK-293	Rosuvastatin	0.28	0.37	1.3	Zhang et al., 2019
	Cyclosporin A	HEK-293	E17βG	1.0	0.87	0.9	Shen et al., 2013;
		HEK-293	Rosuvastatin	0.28	0.21	0.8	Shen et al., 2015
		HEK-293	Pitavastatin	0.027	0.025	0.9	Takahashi et al., 2016
	Estropipate	HEK-293	Rosuvastatin	0.07	0.05	0.7	Zhang et al., 2019
	Estrone 3 sulfate	HEK-293	Rosuvastatin	0.10	0.12	1.2	Zhang et al., 2019
	Ritonavir	HEK-293	E17βG	0.49	1.3	2.7	Shen et al., 2013;
	Gemfibrozil	HEK-293	E17βG	20.2	41.4	2.0	Shen et al., 2013;
	Verapamil	HEK-293	E17βG	13.5	14.8	1.1	Shen et al., 2013;
	Saquinavir	HEK-293	E17βG	2.9	1.6	0.6	Shen et al., 2013;
OATP1B3	Rifampin	HEK-293	CCK-8	1.4	0.46	0.3	Shen et al., 2013;
		HEK-293	Rosuvastatin	1.7	0.49	0.3	Shen et al., 2013;
		HEK-293	E17βG	1.6	0.2	0.1	Chu et al., 2015
		HEK-293	Rosuvastatin	1.0	0.69	0.7	Zhang et al., 2019
	Rifamycin SV	HEK-293	Rosuvastatin	0.45	0.24	0.5	Zhang et al., 2019
	Cyclosporin A	HEK-293	CCK-8	0.50	0.80	1.6	Shen et al., 2013;
		HEK-293	Rosuvastatin	0.25	0.13	0.5	Shen et al., 2015

	Estropipate	HEK-293	Rosuvastatin	12.0	11.1	0.9	Zhang et al., 2019
	Estrone 3 sulfate	HEK-293	Rosuvastatin	23.4	21.3	0.9	Zhang et al., 2019
	Ritonavir	HEK-293	CCK-8	1.3	4.0	3.1	Shen et al., 2013;
	Gemfibrozil	HEK-293	CCK-8	22.4	50.1	2.2	Shen et al., 2013;
	Verapamil	HEK-293	CCK-8	52.7	87.3	1.7	Shen et al., 2013;
	Saquinavir	HEK-293	CCK-8	3.6	5.5	1.5	Shen et al., 2013;
OATP2B1	Rifampin	HEK-293	E3S	69.1	40.1	0.6	Shen et al., 2013;
		HEK-293	Rosuvastatin	81.6	89.8	1.1	Shen et al., 2013;
		HEK-293	Rosuvastatin	82.3	78.2	1.0	Zhang et al., 2019
	Rifamycin SV	HEK-293	Rosuvastatin	4.4	3.8	0.9	Zhang et al., 2019
	Cyclosporin A	HEK-293	E3S	>50	>50		Shen et al., 2013;
	Estropipate	HEK-293	Rosuvastatin	11.8	8.6	0.7	Zhang et al., 2019
	Estrone 3 sulfate	HEK-293	Rosuvastatin	11.4	13.2	1.2	Zhang et al., 2019
	Ritonavir	HEK-293	E3S	4.5	10.7	2.4	Shen et al., 2013;
	Gemfibrozil	HEK-293	E3S	>100	>100		Shen et al., 2013;
	Verapamil	HEK-293	E3S	>200	>200		Shen et al., 2013;
	Saquinavir	HEK-293	E3S	12.3	9.4	0.8	Shen et al., 2013;
OATPs & NTCP	Rifampin	Hepatocytes	Rosuvastatin	0.28	0.90	3.2	Shen et al., 2013;
		Hepatocytes	Pitavastatin	0.7	1.1	1.6	Takahashi et al.,2013 and 2016
	Cyclosporin A	Hepatocytes	Rosuvastatin	0.29	0.30	1.0	Shen et al., 2015
		Hepatocytes	Pitavastatin	1.0	0.9	0.9	Takahashi et al., 2013 and 2016
NTCP	Rifampin	HEK-293	TCA	35.1	277	7.9	Chu et al., 2015
		HEK-293	Rosuvastatin	>300	127		Zhang et al., 2019
	Cyclosporin A	HEK-293	Rosuvastatin	3.9	2.1	0.5	Shen et al., 2015
	Rifamycin SV	HEK-293	Rosuvastatin	54.0	59.3	1.1	Zhang et al., 2019
	Estropipate	HEK-293	Rosuvastatin	20.5	14.8	0.7	Zhang et al., 2019
	Estrone 3 sulfate	HEK-293	Rosuvastatin	23.6	19.5	0.8	Zhang et al., 2019
OCT2	Pyrimethamine	HEK-293	Metformin	1.2	4.1	3.4	Shen et al., 2016

	Cimetidine	HEK-293	Metformin	167	200	1.2	Shen et al., 2016
	Quinidine	HEK-293	Metformin	19.4	19.5	1.0	Shen et al., 2016
	Vandetanib	HEK-293	Metformin	3.3	7.7	2.3	Shen et al., 2016
	Ketoconazole	HEK-293	Metformin	0.92	1.6	1.7	Shen et al., 2016
	Imipramine	HEK-293	Metformin	12.3	2.1	0.2	Shen et al., 2016
MATE1	Pyrimethamine	HEK-293	Metformin	0.17	0.11	0.6	Shen et al., 2016
	Cimetidine	HEK-293	Metformin	4.9	2.3	0.5	Shen et al., 2016
	Quinidine	HEK-293	Metformin	22.0	9.9	0.5	Shen et al., 2016
	Vandetanib	HEK-293	Metformin	1.4	0.46	0.3	Shen et al., 2016
	Ketoconazole	HEK-293	Metformin	2.7	1.1	0.4	Shen et al., 2016
	Imipramine	HEK-293	Metformin	48.4	37.5	0.8	Shen et al., 2016
MATE2-K	Pyrimethamine	HEK-293	Metformin	0.25	0.15	0.6	Shen et al., 2016
	Cimetidine	HEK-293	Metformin	32.2	13.5	0.4	Shen et al., 2016
	Quinidine	HEK-293	Metformin	18.5	5.2	0.3	Shen et al., 2016
	Vandetanib	HEK-293	Metformin	0.45	0.30	0.7	Shen et al., 2016
	Ketoconazole	HEK-293	Metformin	25.0	23.5	0.9	Shen et al., 2016
	Imipramine	HEK-293	Metformin	73.5	76.0	1.0	Shen et al., 2016
P-gp	Elacridar	Membrane vesicles	N-methyl quinidine	0.6	0.09	0.2	Kosa et al., 2018
	PSC833	Membrane vesicles	N-methyl quinidine	0.024	0.03	1.3	Kosa et al., 2018
BCRP	Rifampin	Membrane vesicles	Rosuvastatin	79	14	0.2	Kosa et al., 2018
	Elacridar	Membrane vesicles	Rosuvastatin	0.16	0.5	3.1	Kosa et al., 2018
	KO143	Membrane vesicles	Rosuvastatin	0.19	1	5.3	Kosa et al., 2018
MRP2	Rifampin	Membrane vesicles	EASG	118	14.7	0.1	Chu et al., 2015

Note: HEK-293, human embryonic kidney 293 cells; IC_{50}, half-maximal inhibitory concentration; BCRP, breast cancer resistance protein; MATE, multidrug and toxin extrusion; MRP, multidrug resistance-associated protein; NTCP, sodium-taurocholate co-transporting polypeptide; OAT, organic anion transporter; OATP, organic anion transporting polypeptide; OCT, organic cation transporter; P-gp, P-glycoprotein. EASG, ethacrynic acid glutathione conjugate.

Table 5. Summary of some literature describing transporter DDIs in cynomolgus monkeys and humans.

Transporter	Probe	Inhibitor	Species	Probe Dose Regimen	Inhibitor Dose Regimen	AUCR	CL_R Ratio	Reference
OATP1B1 and OATP1B3	Rosuvastatin	Rifampin	Cynomolgus monkey	Rosuvastatin 1 mpk, sd, iv	Rifampin 18 mpk, sd, po	2.7	ND	Chu et al. 2015
				Rosuvastatin 0.5 mpk cassette), sd, iv	Rifampin 20 mpk, sd, po	2.3	ND	Cheng et al., 2021
				Rosuvastatin 3 mpk, sd, po	Rifampin 15 mpk, sd, po	2.9	ND	Shen et al. 2013
				Rosuvastatin 3 mpk, sd, po	Rifampin 18 mpk, sd, po	4.9	ND	Chu et al. 2015
				Rosuvastatin 3 mpk, sd, po	Rifampin 30 mpk, sd, po	3.4	ND	Zhang et al. 2019
				Rosuvastatin 1 mpk cassette), sd, po	Rifampin 30 mpk, sd, po	21.3	1.4	Kosa et al., 2018
				Rosuvastatin 2 mpk cassettet), sd, po	Rifampin 1 mpk, sd, po	1.7	ND	Ufuk et al., 2018
				Rosuvastatin 2 mpk (cassette t), sd, po	Rifampin 3 mpk, sd, po	9.0	ND	Ufuk et al., 2018
				Rosuvastatin 2 mpk (cassette), sd, po	Rifampin 10 mpk, sd, po	13.6	ND	Ufuk et al., 2018
				Rosuvastatin 2 mpk (cassette), sd, po	Rifampin 30 mpk, sd, po	19.4	ND	Ufuk et al., 2018
			Human	Rosuvastatin 5 mg, sd, po	Rifampin 600 mg, sd, iv	3.3	ND	Prueksaritanont et al. 2014
				Rosuvastatin 5 mg, sd, po	Rifampin 600 mg, sd, po	4.4	ND	Prueksaritanont et al. 2014
				Rosuvastatin 20 mg, sd, po	Rifampin 600 mg, sd, iv	3.3	ND	Wu et al. 2017
				Rosuvastatin 5 mg, sd, po	Rifampin 600 mg, sd, po	4.8	1.0	Shen et al., 2016
				Rosuvastatin 0.5 mg (cocktail), sd, po	Rifampin 300 mg, sd, po	2.2	ND	Takehara et al. 2018
				Rosuvastatin 0.5 mg (cocktail), sd, po	Rifampin 600 mg, sd, po	2.4	ND	Takehara et al. 2018
				Rosuvastatin 10 mg (cocktail), sd, po	Rifampin 600 mg, sd, po	3.5	ND	Wiebe et al. 2020
				Rosuvastatin 5 mg (cocktail), sd, po	Rifampin 150 mg, sd, po	1.6	ND	Mori et al. 2020
				Rosuvastatin 5 mg (cocktail), sd, po	Rifampin 300 mg, sd, po	2.3	ND	Mori et al. 2020
				Rosuvastatin 5 mg (cocktail), sd, po	Rifampin 600 mg, sd, po	2.5	ND	Mori et al. 2020
				Rosuvastatin 50 μg (cocktail), sd, po	Rifampin 600 mg, sd, po	3.6	0.75	Tatosian et al. 2021
		Cyclosporin A	Cynomolgus monkey	Rosuvastatin 3 mpk, sd, po	Cyclosporin A 100 mpk, sd, po	6.3	ND	Shen et al., 2015

		Human	Radiolabeled rosuvastatin (0.91-2.57 µg), sd iv	Cyclosporin A 2.5 mg/kg/hr, iv infusion	1.4	ND	Billington et al. 2019
			Rosuvastatin 10 or 20 mg, md, po	Cyclosporin A 75 to 200 mg, md, po	7.1	ND	Simonson et al. 2004
	Probenecid	Cynomolgus monkey	Rosuvastatin 1 mpk cassette), sd, po	Probenecid 30 mpk, sd, po	2.6	7.8	Kosa et al., 2018
		Human	Rosuvastatin 10 mg (cocktail), sd, po	Probenecid 1000 mg, sd, po	2.2	ND	Wiebe et al. 2020
Atorvastatin	Rifampin	Cynomolgus monkey	Atorvastatin 1 mpk, sd, iv	Rifampin 18 mpk, sd, po	1.7	ND	Chu et al. 2015
			Atorvastatin 5 mpk, sd, po	Rifampin 18 mpk, sd, po	1.7	ND	Chu et al. 2015
		Human	Atorvastatin 1 mg (cocktail), sd, po	Rifampin 300 mg, sd, po	4.2	ND	Takehara et al. 2018
			Atorvastatin 1 mg (cocktail), sd, po	Rifampin 600 mg, sd, po	6.1	ND	Takehara et al. 2018
			Atorvastatin 5 mg (cocktail), sd, po	Rifampin 150 mg, sd, po	3.4	ND	Mori et al. 2020
			Atorvastatin 5 mg (cocktail), sd, po	Rifampin 300 mg, sd, po	4.9	ND	Mori et al. 2020
			Atorvastatin 5 mg (cocktail), sd, po	Rifampin 600 mg, sd, po	7.3	ND	Mori et al. 2020
			Atorvastatin 100 µg (cocktail), sd, po	Rifampin 600 mg, sd, po	6.1	ND	Tatosian et al. 2021
Pitavastatin	Rifampin	Cynomolgus monkey	Pitavastatin 0.3 mpk, sd, iv	Rifampin 20 mpk, sd, po	3.6	ND	Takahashi et al., 2013
			Pitavastatin 0.3 mpk, sd, po	Rifampin 20 mpk, sd, po	14.8	ND	Takahashi et al., 2013
			Pitavastatin 0.2 mpk, sd, iv	Rifampin 1 mpk, sd, po	1.2	ND	Thakare et al., 2017
			Pitavastatin 0.2 mpk, sd, iv	Rifampin 3 mpk, sd, po	2.4	ND	Thakare et al., 2017
			Pitavastatin 0.2 mpk, sd, iv	Rifampin 10 mpk, sd, po	3.8	ND	Thakare et al., 2017
			Pitavastatin 0.2 mpk, sd, iv	Rifampin 30 mpk, sd, po	4.5	ND	Thakare et al., 2017
			Pitavastatin 1 mpk cassette), sd, po	Rifampin 30 mpk, sd, po	39	1.0	Kosa et al., 2018
			Pitavastatin 2 mpk (cassette), sd, po	Rifampin 1 mpk, sd, po	1.3	ND	Ufuk et al., 2018
			Pitavastatin 2 mpk (cassette), sd, po	Rifampin 3 mpk, sd, po	4.7	ND	Ufuk et al., 2018
			Pitavastatin 2 mpk (cassette), sd, po	Rifampin 10 mpk, sd, po	9.4	ND	Ufuk et al., 2018
			Pitavastatin 2 mpk (cassette), sd, po	Rifampin 30 mpk, sd, po	15.0	ND	Ufuk et al., 2018
			Pitavastatin <1 mpk (cassette), sd, po	Rifampin 30 mpk, sd, po	5.3	ND	Eng et al., 2021
		Human	Pitavastatin 0.2 mg (cocktail), sd, po	Rifampin 300 mg, sd, po	2.3	ND	Takehara et al. 2018
			Pitavastatin 0.2 mg (cocktail), sd, po	Rifampin 600 mg, sd, po	2.8	ND	Takehara et al. 2018
			Pitavastatin 2 mg (cocktail), sd, po	Rifampin 150 mg, sd, po	2.5	ND	Mori et al. 2020

			Pitavastatin 2 mg (cocktail), sd, po	Rifampin 300 mg, sd, po	3.5	ND	Mori et al. 2020
			Pitavastatin 2 mg (cocktail), sd, po	Rifampin 600 mg, sd, po	4.0	ND	Mori et al. 2020
			Pitavarstatin 10 µg (cocktail), sd, po	Rifampin 600 mg, sd, po	3.7	ND	Tatosian et al. 2021
	Cyclosporin A	Cynomolgus monkey	Pitavastatin 0.3 mpk, sd, iv	Cyclosporin A 100 mpk, sd, po	3.2	ND	Takahashi et al., 2013
			Pitavastatin 0.3 mpk, sd, po	Cyclosporin A 100 mpk, sd, po	10.6	ND	Takahashi et al., 2013
		Human	Pitavastatin 2 mg, md, po	Cyclosporin A 2 mg/kg, sd, po	4.5	ND	NDA 022363
CPI	Rifampin	Cynomolgus monkey	Endogenous compound	Rifampin 15 mpk, sd, po	2.6	1.6	Shen et al. 2016
			Endogenous compound	Rifampin 18 mpk, sd, po	4.5	ND	Takehara et al. 2019
			Endogenous compound	Rifampin 20 mpk, sd, po	5.4	ND	Cheng et al. 2021
		Human	Endogenous compound	Rifampin 600 mg, sd, po	4.0	0.89	Shen et al., 2017
			Endogenous compound	Rifampin 600 mg, sd, po	3.3	ND	Shen et al., 2018
			Endogenous compound	Rifampin 300 mg, sd, po	3.0	ND	Takehara et al. 2018
			Endogenous compound	Rifampin 600 mg, sd, po	4.6	ND	Takehara et al. 2018
			Endogenous compound	Rifampin 150 mg, sd, po	1.5	ND	Mori et al. 2020
			Endogenous compound	Rifampin 300 mg, sd, po	2.3	ND	Mori et al. 2020
			Endogenous compound	Rifampin 600 mg, sd, po	3.7	ND	Mori et al. 2020
			Endogenous compound	Rifampin 600 mg, sd, po	4.4	0.79	Tatosian et al. 2021
	Cyclosporin A	Cynomolgus monkey	Endogenous compound	Cyclosporin A 100 mpk, sd, po	2.6	1.3	Shen et al. 2016
			Endogenous compound	Cyclosporin A 4 mpk, sd, po	1.1	ND	Gu et al. 2020
			Endogenous compound	Cyclosporin A 20 mpk, sd, po	1.4	ND	Gu et al. 2020
			Endogenous compound	Cyclosporin A 100 mpk, sd, po	4.4	ND	Gu et al. 2020
		Human	Endogenous compound	Cyclosporin A 2.5 mg/kg/hr, iv infusion	3.0	ND	Billington et al. 2019
			Endogenous compound	Cyclosporin A 100 mg, sd, po	1.7	ND	Lee et al. 2019
	Probenecid	Cynomolgus monkey	Endogenous compound	Probenecid 40 mpk, sd, po	0.78	ND	Gu et al. 2020
			Endogenous compound	Probenecid 40 mpk (po) and furosemide 2 mpk (iv), sd	0.89	ND	Gu et al. 2020
		Human	Endogenous compound	Probenecid 1000 mg, sd, po	1.39	0.97	Zhang et al. 2020

				Endogenous compound	Probenecid 1000 mg and furosemide 40 mg, sd, po	1.58	1.23	Zhang et al. 2020
	CPIII	Rifampin	Cynomolgus monkey	Endogenous compound	Rifampin 15 mpk, sd, po	3.6	0.79	Shen et al. 2016
				Endogenous compound	Rifampin 18 mpk, sd, po	5.0	ND	Takehara et al. 2019
				Endogenous compound	Rifampin 20 mpk, sd, po	8.8	ND	Cheng et al. 2021
			Human	Endogenous compound	Rifampin 600 mg, sd, po	3.5	0.38	Lai et al. 2016 and Shen et al., 2017
				Endogenous compound	Rifampin 600 mg, sd, po	2.6	ND	Shen et al., 2018
				Endogenous compound	Rifampin 600 mg, sd, po	2.7	0.38	Tatosian et al. 2021
		Cyclosporin A	Cynomolgus monke	Endogenous compound	Cyclosporin A 100 mpk, sd, po	5.0	0.28	Shen et al. 2016
				Endogenous compound	Cyclosporin A 4 mpk, sd, po	1.1	ND	Gu et al. 2020
				Endogenous compound	Cyclosporin A 20 mpk, sd, po	1.8	ND	Gu et al. 2020
				Endogenous compound	Cyclosporin A 100 mpk, sd, po	4.6	ND	Gu et al. 2020
			Human	Endogenous compound	Cyclosporin A 2.5 mg/kg/hr, iv infusion	3.8	ND	Billington et al. 2019
				Endogenous compound	Cyclosporin A 100 mg, sd, po	1.9	ND	Lee et al. 2019
		Probenecid	Cynomolgus monkey	Endogenous compound	Probenecid 40 mpk, sd, po	1.5	ND	Shen et al. 2018
				Endogenous compound	Probenecid 40 mpk (po) and furosemide 2 mpk (iv), sd	1.9	ND	Shen et al. 2018
			Human	Endogenous compound	Probenecid 1000 mg, sd, po	1.34	1.34	Zhang et al. 2020
				Endogenous compound	Probenecid 1000 mg and furosemide 40 mg, sd, po	1.34	1.51	Zhang et al. 2020
BCRP	Sulfasalazine	Curcumin	Cynomolgus monkey	Sulfasalazine 5 mpk (cassesset), sd, po	Curcumin 30 mpk, sd, po	2.9	ND	Karibe et al., 2018
			Human	Sulfasalazine 100 µg, sd, po	Curcumin 2000 mg, sd, po	2.0	ND	Kusuhara et al. 2012
				Sulfasalazine 2000 mg, sd, po	Curcumin 2000 mg, sd, po	3.2	ND	Kusuhara et al. 2012
		Pantoprazole	Cynomolgus monkey	Sulfasalazine 5 mpk (cassette), sd, po	Pantoprazole 20 mpk, sd, po	1.6	ND	Karibe et al., 2018
			Human	Sulfasalazine 500 mg, sd, po	Pantoprazole 40 mg, sd, po	1.8	ND	Adkison et al. 2009

OAT1 and OAT3	Furosemide	Probenecid	Cynomolgus monkey	Furosemide 2 mpk, sd, iv	Probenecid 40 mpk, sd, iv	4.1	0.12	Shen et al., 2018
			Human	Furosemide 40 mg, sd, iv	Probenecid 1000 mg, sd, iv	3.1	0.20	Smith et al., 1980
				Furosemide 80 mg, sd, po	Probenecid 1000 mg, sd, po	2.7	0.34	Vree et al., 1995
				Furosemide 40 mg, sd, po	Probenecid 1000 mg, sd, po	3.3	0.23	Shen et al., 2018
				Furosemide 1 mg (cocktail), sd, po	Probenecid 1000 mg, sd, po	2.7	ND	Wiebe et al. 2020
	Pyridoxic acid	Probenecid	Cynomolgus monkey	Endogenous compound	Probenecid 40 mpk, sd, iv	2.8	0.10	Shen et al., 2018
				Endogenous compound	Probenecid 40 mpk and furosemide 2 mpk, sd, iv	2.9	0.39	Shen et al., 2018
			Human	Endogenous compound	Probenecid 1000 mg, sd, po	3.1	0.37	Shen et al., 2018
				Endogenous compound	Probenecid 1000 mg and furosemide 40 mg, sd, po	3.2	0.40	Shen et al., 2018
	Famotidine	Probenecid	Cynomolgus monkey	Famotidine 0.3 mpk, sd, iv	Probenecid 22.5 mpk, sd, iv	2.1	0.36	Tahara et al., 2006
			Human	Famotidine 20 mg, sd, po	Probenecid 1500 mg and furosemide 40 mg, sd, po	1.8	0.36	Inotsume et al., 1999
OCT2, MATE1, and MATE2-K	Metformin	Pyrimethamine	Cynomolgus monkey	Metformin 3.9 mpk, sd, iv	Pyrimethamine 0.5 mpk, sd, iv	2.2	0.45[d]	Shen et al., 2016
			Human	Metformin 250 mg, sd, po	Pyrimethamine 50 mg, sd, po	1.4	0.65	Kusuhara et al., 2011
				Metformin 100 μg, sd, po	Pyrimethamine 50 mg, sd, po	1.1	0.72	Kusuhara et al., 2011
				Metformin 750/500 mg, sd, po	Pyrimethamine 50 mg, sd, po	2.7	0.28	Oh et al., 2015

Note: DDI, drug-drug interaction; BCRP, breast cancer resistance protein; MATE, multidrug and toxin extrusion; MRP, multidrug resistance-associated protein; NTCP, sodium-taurocholate co-transporting polypeptide; OAT, organic anion transporter; OATP, organic anion transporting polypeptide; OCT, organic cation transporter; P-gp, P-glycoprotein.

DMD Fast Forward. Published on December 10, 2021 as DOI: 10.1124/dmd.121.000695
This article has not been copyedited and formatted. The final version may differ from this version.

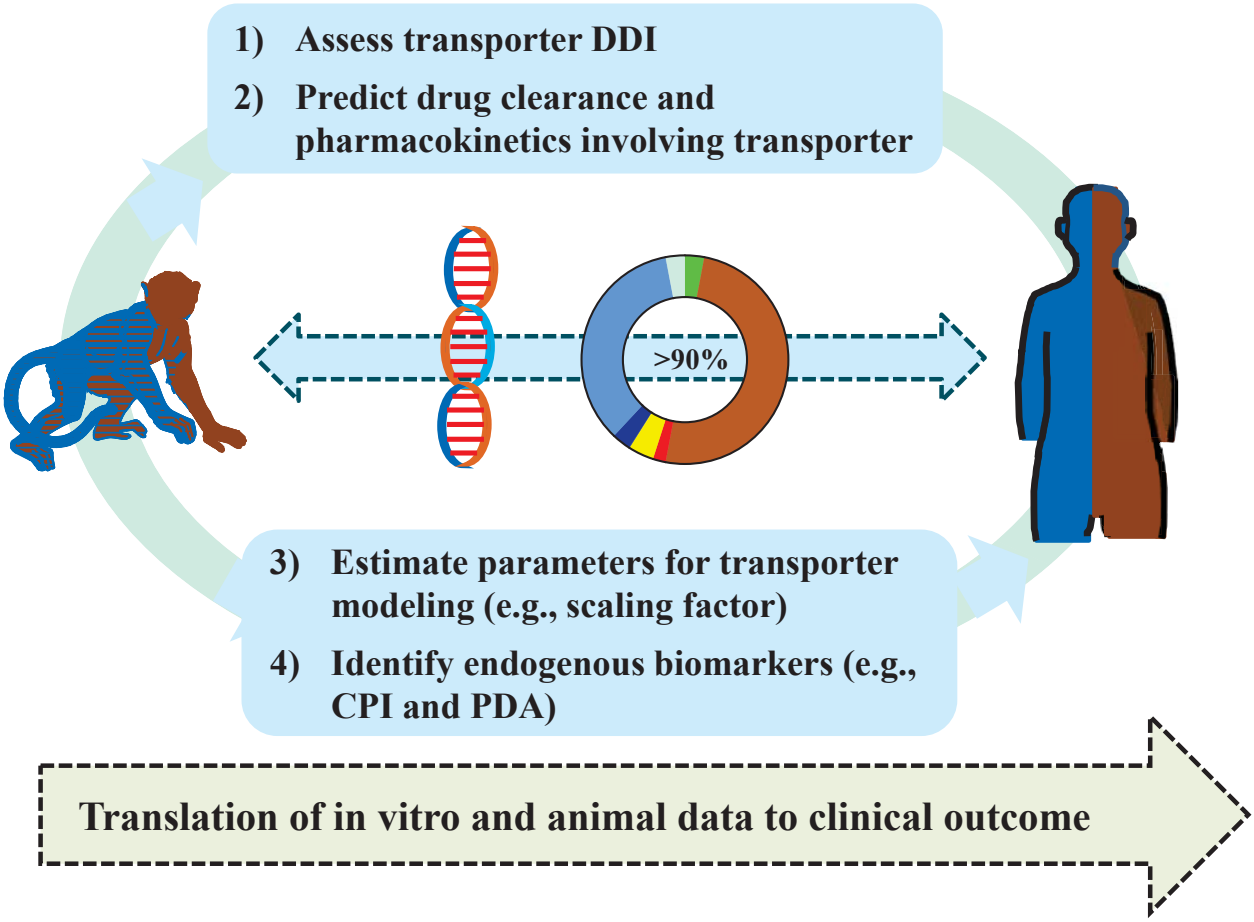

Figure 1

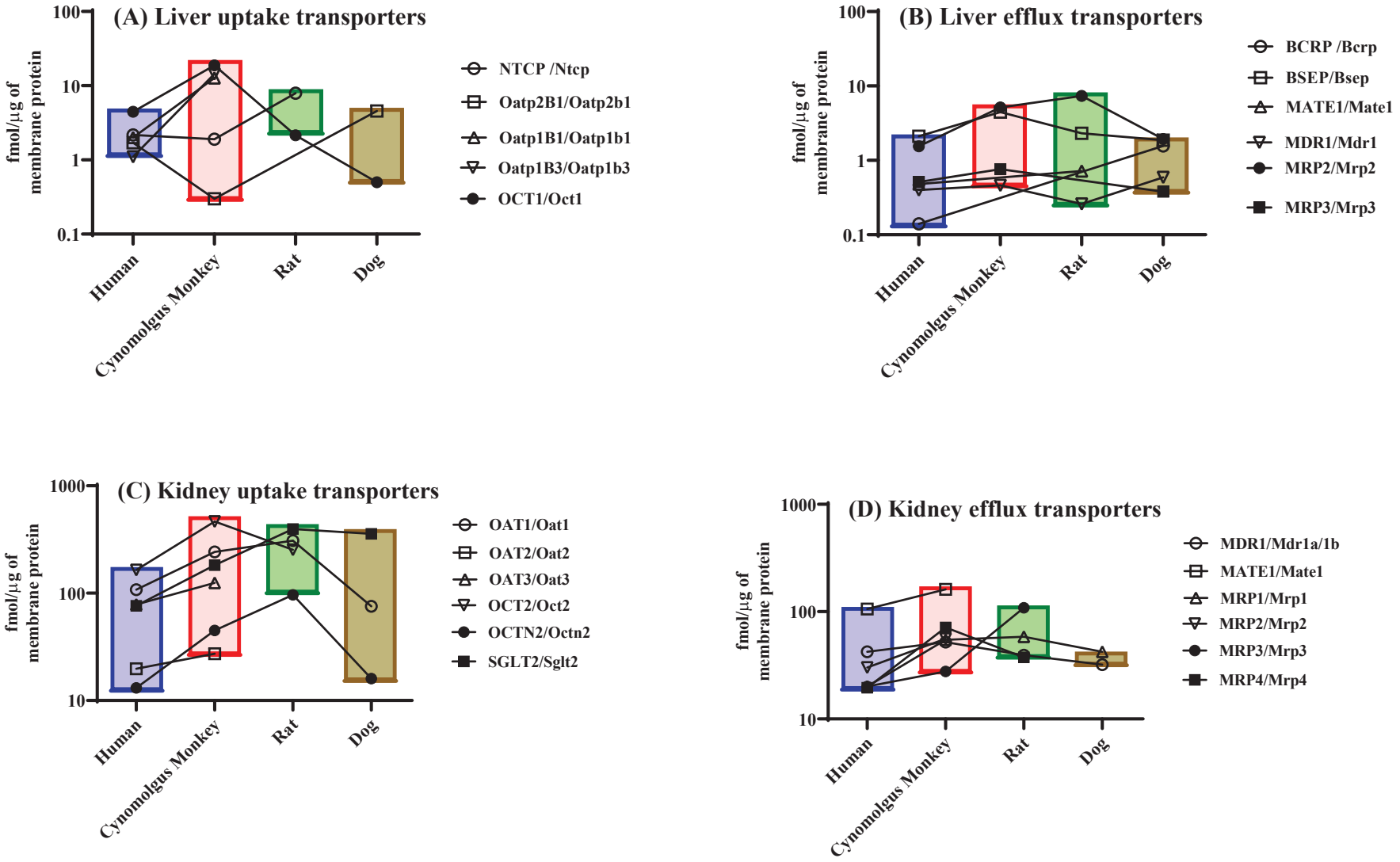
(A) Liver uptake transporters
fmol/μg of membrane protein
100
10
1
0.1
Human
Cynomolgus Monkey
Rat
Dog
NTCP /Ntcp
Oatp2B1/Oatp2b1
Oatp1B1/Oatp1b1
Oatp1B3/Oatp1b3
OCT1/Oct1
(B) Liver efflux transporters
BCRP /Bcrp
BSEP/Bsep
MATE1/Mate1
MDR1/Mdr1
MRP2/Mrp2
MRP3/Mrp3
(C) Kidney uptake transporters
1000
OAT1/Oat1
OAT2/Oat2
OAT3/Oat3
OCT2/Oct2
OCTN2/Octn2
SGLT2/Sglt2
(D) Kidney efflux transporters
MDR1/Mdr1a/1b
MATE1/Mate1
MRP1/Mrp1
MRP2/Mrp2
MRP3/Mrp3
MRP4/Mrp4

Figure 2

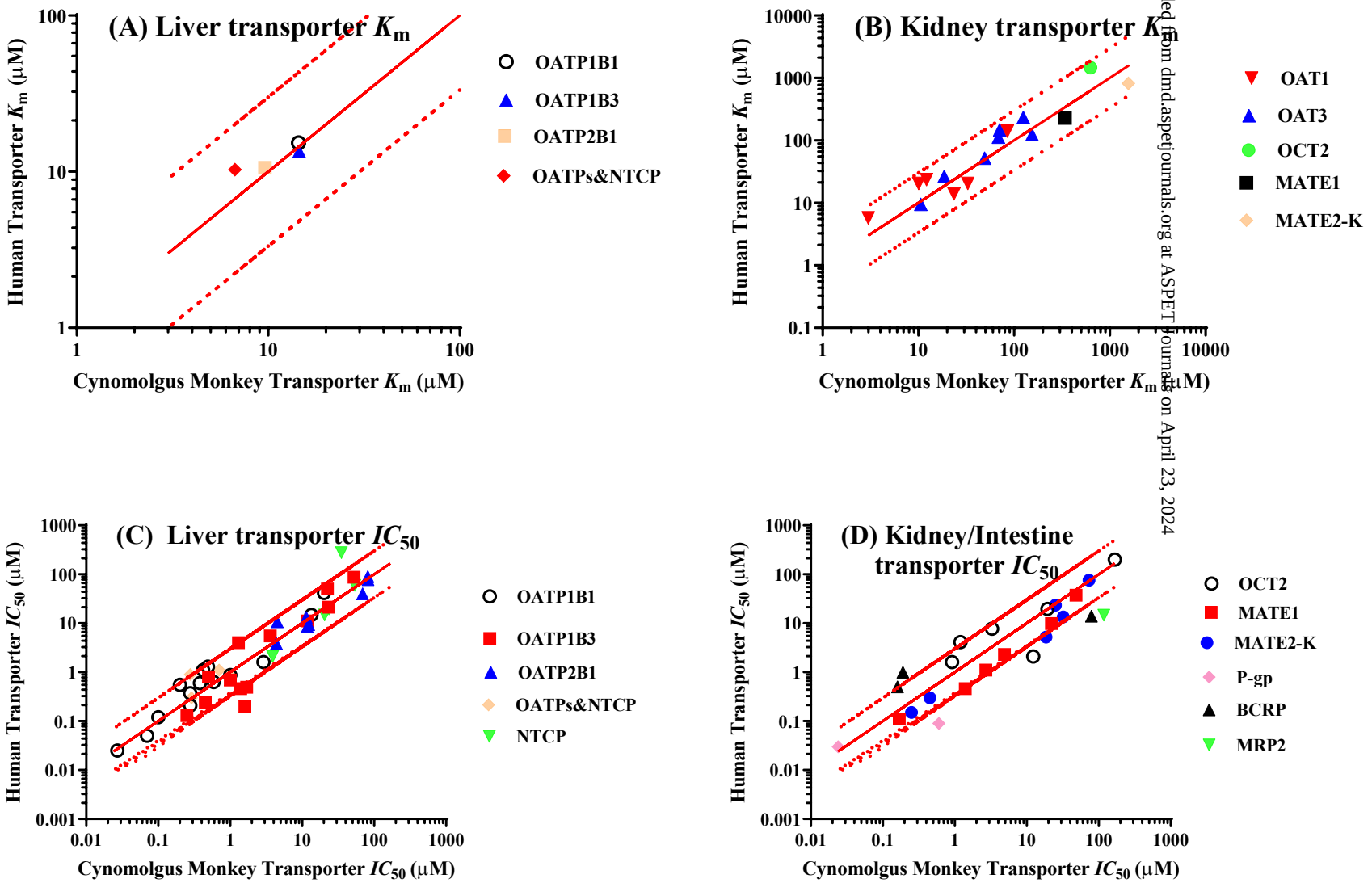

Figure 3

DMD Fast Forward. Published on December 10, 2021 as DOI: 10.1124/dmd.121.000695
This article has not been copyedited and formatted. The final version may differ from this version.

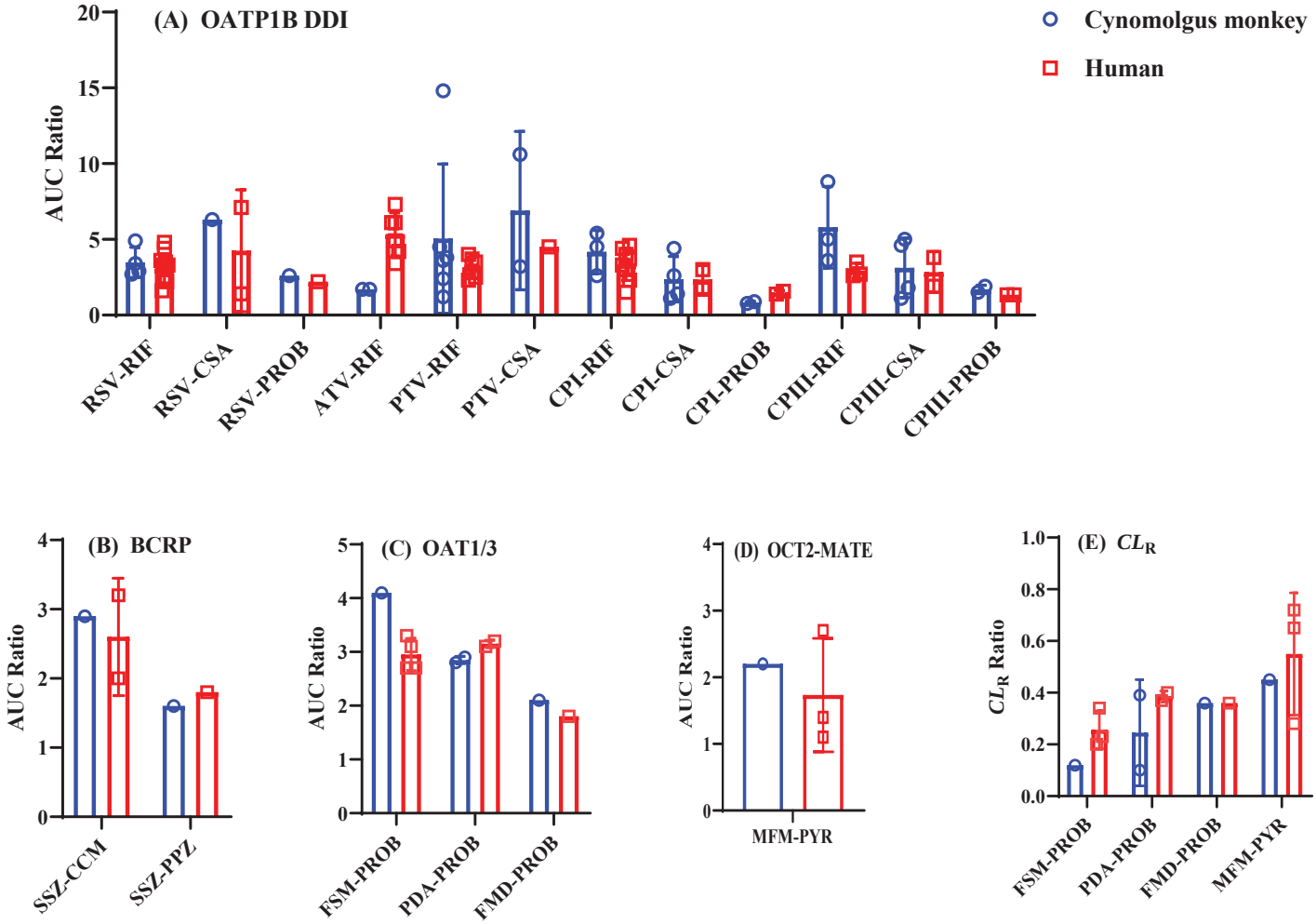

Figure 4